The Effect of Non-Steroidal Anti-Inflammatory Drugs on Canine Transitional Cell Carcinoma and Its Correlation with Cyclooxygenase-2 Expression

by
Marcus Andrew Weinman

A PROJECT

submitted to

Oregon State University

University Honors College

in partial fulfillment of
the requirements for the
degree of

Honors Baccalaureate of Science in Microbiology
(Honors Scholar)

Presented May 21st, 2015
Commencement June 2015

AN ABSTRACT OF THE THESIS OF

Marcus Andrew Weinman for the degree of Honors Baccalaureate of Science in Microbiology presented on May 21st, 2015. Title: The Effects of Non-Steroidal Anti-Inflammatory Drugs on Canine Transitional Cell Carcinoma and Its Correlation with Cyclooxygenase-2 Expression.

Abstract approved:

Shay Bracha

Canine transitional cell carcinoma (TCC) has been shown to have a substantial inflammatory component. It exhibits genotypic and morphologic elements that resemble its human counterpart. Cyclooxygenases (COX) are key enzymes in the synthesis of proinflammatory molecules, such as prostaglandins. Excess prostaglandin production through cyclooxygenases may promote oncogenesis and progression of certain cancers. Inhibition of COX-2 represents a therapeutic target for clinicians treating several cancers, including canine TCC. With most traditional NSAIDs, gastrointestinal side effects are concerning. Firocoxib, a novel second-generation NSAID, exhibits 350-430 fold selectivity for COX-2 and is approved for veterinary use, including treatment of canine TCC. To understand the effects of Firocoxib *in vitro*, we evaluated the cyclooxygenase profile for 5 TCC cell lines, as well as primary tissue samples from patients diagnosed with TCC. All cell lines expressed *ptgs-2*; TCC tissue samples varied in their *ptgs-2* expression. Changes in prostaglandin E_2 (PGE_2) concentration, angiogenic factors, oxidative stress, *ptgs-2* expression, and the proteome after Firocoxib treatment were investigated. Two TCC cell lines were treated with Firocoxib in cell proliferation assays to investigate metabolic effects of COX-2 inhibition. Significant decreases in PGE_2 concentrations after Firocoxib treatment were noticed, despite high basal PGE_2 production. Unique proteomic changes were discovered.

Key words: COX-2, NSAID, Firocoxib, TCC, Prostaglandin E_2

Corresponding email address: weinmanm@onid.orst.edu, mw140000@gmail.com

The Effect of Non-Steroidal Anti-Inflammatory Drugs on Canine Transitional Cell Carcinoma and Its Correlation with Cyclooxygenase-2 Expression

by
Marcus Andrew Weinman

A PROJECT

submitted to

Oregon State University

University Honors College

in partial fulfillment of
the requirements for the
degree of

Honors Baccalaureate of Science in Microbiology
(Honors Scholar)

Presented May 21st, 2015
Commencement June 2015

Honors Baccalaureate of Science in Microbiology project of Marcus Andrew Weinman presented on May 21st, 2015.

APPROVED:

Shay Bracha, Mentor, representing Veterinary Medicine

Patrick Chappell, Committee Member, representing Veterinary Medicine

Siva Kolluri, Committee Member, representing Environmental and Molecular Toxicology

Toni Doolen, Dean, University Honors College

I understand that my project will become part of the permanent collection of Oregon State University. My signature below authorizes release of my project and thesis to any reader upon request.

Marcus A. Weinman, Author

Acknowledgements

I would like to thank Dr. Shay Bracha for his mentorship. His decision to take me under his wing is one I will always be grateful for. His willingness to stick with our project despite the roundabout course it took helped motivate me immensely. Thank you for the freedom you gave me to help shape the outcome of our work. Most importantly, thank you for believing in me.

I would also like to thank Dr. Patrick Chappell for allowing me to work in his lab over the course of the past two years. From the countless pieces of advice to the NWRSS/SfN conferences and everything in-between, your support has been invaluable.

Next, I would like to thank Dr. Claudia Maier for her support throughout my undergraduate research experience. Her mentorship has also helped advance my learning, both in her lab and in others.

I'd like to give special thanks to Cheri Goodall. I've learned so much from you. You're an incredibly valuable resource in the lab; you answer my endless questions, and have been an amazing friend to me. I couldn't have done this without your help and your knowledge.

Finally, I'd like to thank my labmates, my friends, and my family. You've all helped me stay sane during the most insane of times. Your support and encouragement keeps me motivated every day.

1. Introduction

Transitional cell carcinoma (TCC) is the most common type of urinary bladder cancer in dogs.[1] Canine TCC is viewed as an animal model to human TCC since it bears many similarities in etiology, disease course, and response to chemotherapy.[2] Even with chemotherapeutic treatments, survival rates are typically less than one year. The clinical standard of care entails a chemotherapeutic drug (carboplatin, cisplatin, or mitoxantrone) and a non-steroidal inflammatory drug (NSAID). The addition of an NSAID to treatment plans has been shown to increase survival in dogs.[1] This increase is assumed to be due to the inhibition of cyclooxygenase-1 and 2 (COX-1 and COX-2).[1] Transitional cell carcinoma tumors that express both COX-1 and COX-2 in canine bladders have been identified through immunohistochemistry of urinary bladder epithelium.[3] Expression of the COX-2 isoform represents a therapeutic target for clinicians to treat patients with TCC, due to the potential anti-inflammatory and antineoplastic effects of enzyme inhibition.

With recent characterization of both COX enzyme isoforms, an increase in the development of new NSAIDs has followed. Among these second-generation NSAIDs, the coxib family of NSAIDs has been under careful study. Firocoxib is a newer NSAID that has seen clinical use in combination with chemotherapeutic drugs to treat canine TCC, and osteoarthritis.[4,5] Firocoxib possesses a high clinical efficacy due to the 350-fold selectivity of the drug for the COX-2 isoform. This is associated with a large reduction in gastrointestinal side effects typically seen with non-selective NSAIDs.[5,6]

The intent of our study was to investigate the potential of Firocoxib to reduce neoplastic cell viability and inflammation *in vitro*. Characterization of the TCC tumor phenotype is first necessary in order to warrant NSAID treatment. Relative *ptgs-2* (gene encoding the COX-2 protein) expression was examined in both canine TCC cell lines and primary tissue samples from normal bladders and TCC patients. Immunoblotting was performed to detect COX-2 protein present in relation to gene expression. The potential anti-angiogenic effects of Firocoxib treatment were evaluated through quantitation of *vegf, vegfr1, and vegfr2* expression. Cellular oxidative stress was gauged via quantitation of *prdx-1*, *prdx-5*, *prdx-6,* and *sod-1* expression, combined with multiple assays for the generation reactive oxygen species. We also examined the effect of Firocoxib on the production of prostaglandin E_2 (PGE_2) and overall cell proliferation. Mass spectrometry was used to gauge larger effects of Firocoxib treatment on the TCC proteome.

2. Literature Review

Cyclooxygenase enzymes catalyze a committed reaction in the prostaglandin synthesis pathway (Fig. 2.1). Two isoforms, COX-1 and COX-2, have been characterized. COX-1 expression is constitutive and involves homeostatic prostaglandin synthesis, while COX-2 expression can be induced as a response to inflammatory process. The prostaglandin precursor, arachidonic acid, is liberated from membrane glycerophospholipids via phospholipase A2 family of enzymes or diacylglycerol lipase.[7] This allows for COX-1 and COX-2 to oxidize arachidonic acid into prostaglandin G2 (PGG_2), then subsequently reduce PGG_2 to form prostaglandin H_2 (PGH_2).[7] Downstream enzymatic activity (and some non-enzymatic mechanisms) uses PGH_2 as substrate to fully synthesize a variety of prostanoid molecules, most notably PGE_2 and $PGF_{2\alpha}$. These final products of the arachidonic acid cascade can regulate diverse physiological processes, such as immunity, inflammatory response, modification of vascular integrity, and the induction of labor, among others.[8] Modulating prostaglandin synthesis has the potential to affect gastrointestinal and renal homeostasis when treating with NSAIDs.[9]

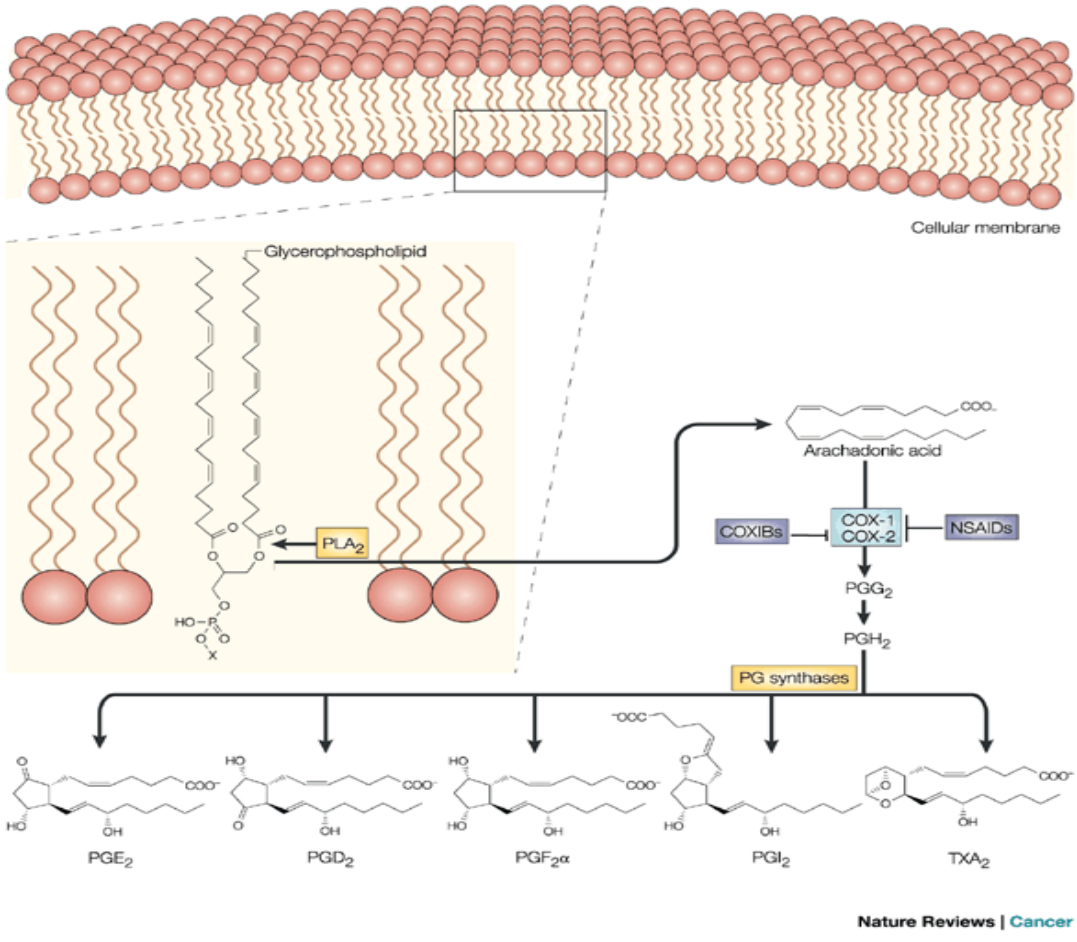

Figure 2.1 - Prostaglandin synthesis pathway. Enzymes in the Phospholipase A2 family free arachidonic acid from membrane glycerophospholipids. COX enzymes then convert arachidonic acid into PGH_2, which serves as the precursor to all prostanoids. Traditional non-selective NSAIDs inhibit both COX enzyme isoforms while molecules in the Coxib family of NSAIDs are specific to COX-2. Figure from Gupta R *et al.*[4]

The COX enzymes have distinct structural properties that dictate their function. Both isoforms contain two active sites that catalyze cyclooxygenase reactions and peroxidase reactions respectively.[10] The cyclooxygenase active site is more clinically relevant due to the use of NSAIDs that inhibit the cyclooxygenase reaction. Both isoforms (COX-1 and COX-2) contain 24 amino acids in the cyclooxygenase active site, but the COX-2 isoform contains a valine substituted for isoleucine at position 523.[10] This property confers the selectivity of COX-2 specific inhibitors to the COX-2 isoform by enlarging the active site (Fig. 2.2).[11] The enlarged active site allows COX-2 to catalyze a wider variety of cyclooxygenase reactions and fit different potential substrates.[12]

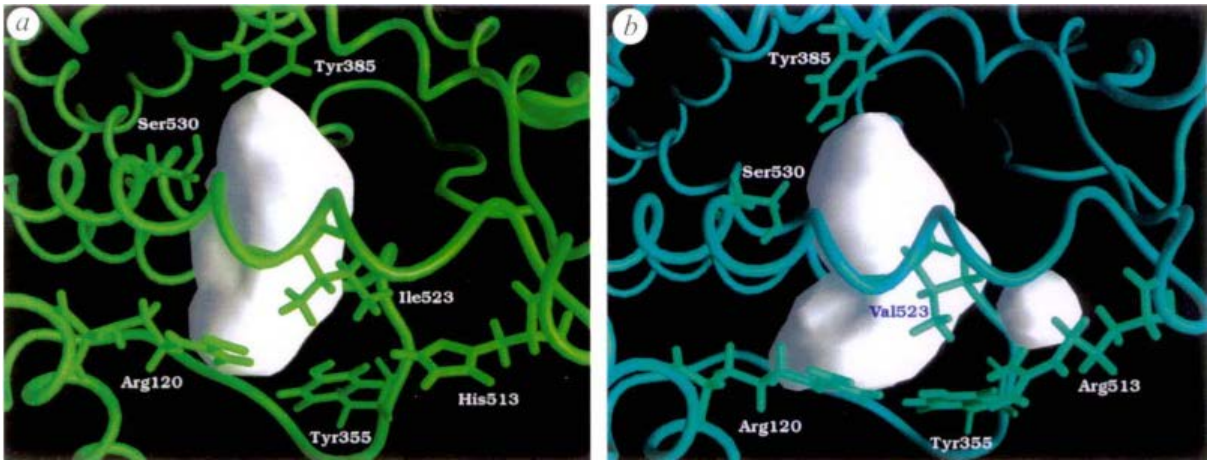

Figure 2.2 – COX-1 and COX-2 cyclooxygenase active sites. Comparison of the accessible molecular surface at NSAID binding sites. (A) Representation of the sheep COX-1 active site with an NSAID (Flurbiprofen) bound. (B) Representation of the human COX-2 active site with a proprietary NSAID bound. Figure adapted from Luong, Christine *et al.*[12]

The role of the COX enzymes in cancer is complex and often multi-faceted. COX-2 is regarded as the inducible isoform of COX-1 and is induced under various stimuli. Many of these stimuli include expression of oncogenes, growth factors (epidermal growth factor), tumor promoting agents (phorbol esters and bile acids), and other pro-inflammatory molecules (TNF-α, bacterial LPS).[13] These stimuli initiate a cell-signaling cascade that results in protein kinase C or mitogen-activated protein kinase activation, which then in turn activates COX-2 transcription (Fig. 2.3). Many transcription factors mediate the expression of *ptgs-2*, such as NF-κB.[10,13] There are various post-transcriptional control mechanisms for *ptgs-2* mRNA that are altered in cancer. Sequences in the 3'-untranslated region (UTR) of *ptgs-2* mRNA are bound by various proteins that increase the mRNA stability, which subsequently increases levels of COX-2 protein in colon cancer cells.[14]

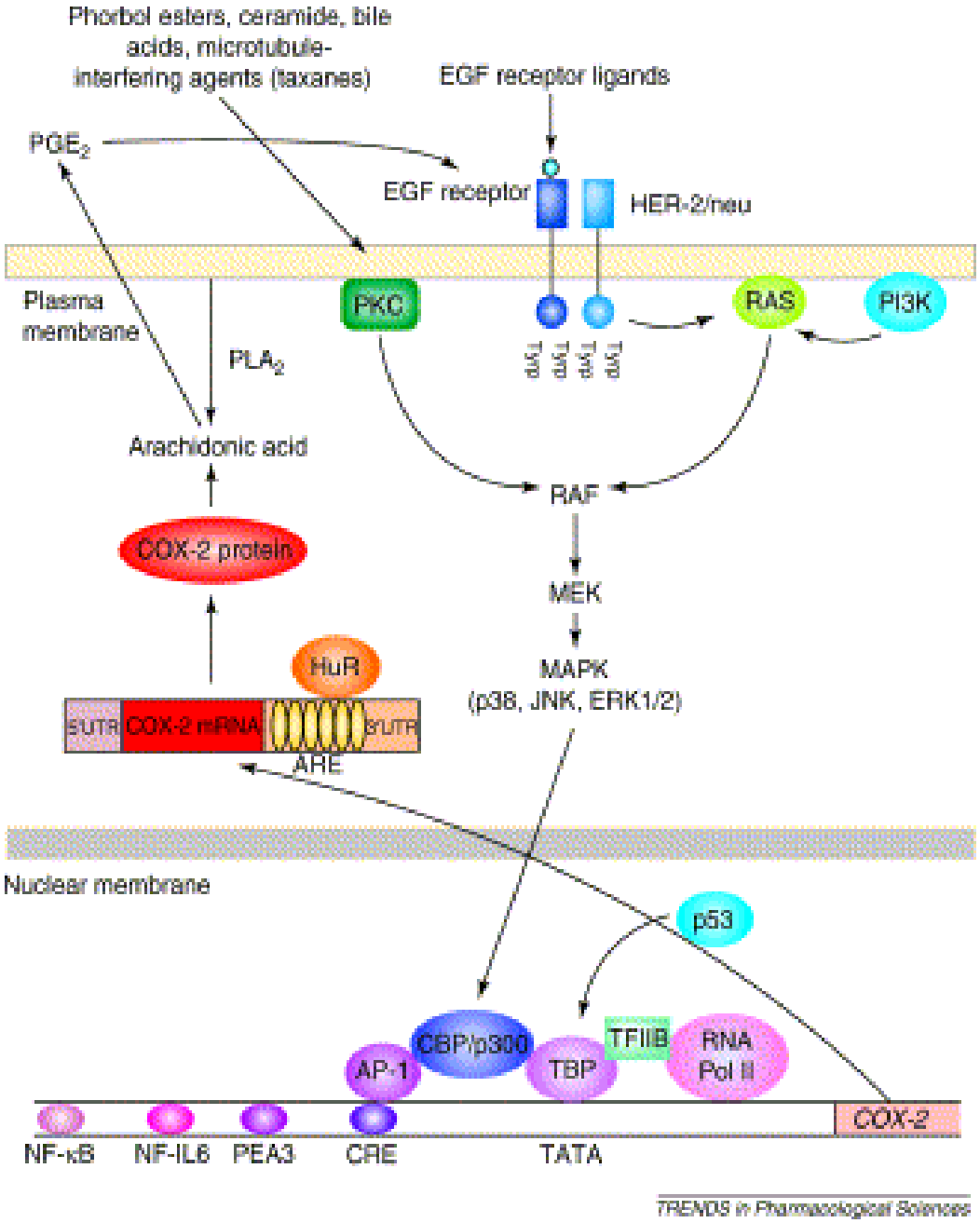

Figure 2.3 – COX-2 activation pathways. Regulation of COX-2 expression in cancer is affected by a wide range of stimuli, including oncogenes, growth factors, tumor promoters, and other molecules. The 3′-untranslated region (3′UTR) of COX-2 mRNA contains a series of sequences (AUUUA) known as AU-enriched elements (AREs) that confer message instability. Augmented binding of HuR, an RNA-binding protein, to these elements is responsible, at least in part, for increased stability of COX-2 mRNA in tumors. Abbreviations: CBP, CREB binding protein; CRE, cAMP response element; ERK, extracellular signal regulated kinase; JNK, Jun N-terminal kinase; MEK, MAPK kinase; NF-IL6, nuclear factor interleukin 6; PEA3, polyomavirus enhancer activator 3; PI3K, phosphatidylinositol 3-kinase; PLA_2, phopholipase A_2; RNA Pol II, RNA polymerase II; TBP, TATA-binding protein. Figure adapted from Dixon, Dan *et al.*[14]

Once expressed, COX-2 can participate directly in carcinogenesis via direct xenobiotic metabolism. Various pro-carcinogens may contain enough substrate specificity for COX-2 for the peroxidase active site and become activated as a consequence.[15,16] Downstream effects of COX-2 expression and increased prostaglandin synthesis also affect different aspects of tumor development and growth. Correlations between increases in COX-2 expression and inhibition of apoptosis have been found in varying tumor types.[17] This includes PGE_2-induced increases in mitogen-associated protein kinase (MAPK) activity, Bcl-2 protein concentration, ras-mediated signal transduction, and disruption of caspase expression.[17] COX-2 eicosanoid products also affect neovascularization of tumors through the mediation of vascular endothelial growth factor (VEGF) expression. Angiogenesis is critical for the growth of tumors, as they require nutrients and oxygen for their growth. In cancer, tumor vasculature possesses a distorted and disorganized structure, which results in the creation of hypoxic conditions and subsequent up-regulation of VEGF.[18] Angiogenic signal is mediated through VEGF binding its cognate receptors, VEGFR-1 and VEGFR-2. Altered tumor vasculature may alter the expression and densities of these receptors. COX-2 inhibition in human familial adenomatous polyposis has resulted in decreases of VEGF mRNA levels.[19] Thromboxane A_2 (TXA_2), a PGH_2 derivative, activates TXA_2-receptor (isoform alpha) and transduces signal that results in VEGF expression.[20] PGE_2 cell signaling also results in an increase in VEGF production and angiogenesis.[17]

COX-2 is also thought to play a role in conferring invasive properties to tumors via up-regulation of matrix metalloproteinases (MMPs), which promotes their extension into the stroma, blood vessels, and overall metastasis. Increased PGE_2 synthesis has been linked to increases in expression of MMP-2 and MMP-9 in human lung and prostate cancers, respectively.[21,22] Increases in MMP production in human prostate cancer was reversible upon treatment with a COX-2 inhibitor.[21] COX-2 production of PGE_2 can also act on immune cells and decrease inflammation. PGE_2 inhibits production of TNF-α in murine macrophages by inducing production of IL-10, which decreases immune response.[23] PGE_2 has also been linked to suppression of B and T-lymphocyte proliferation in human colon cancer patients.[24] PGE_2 also can cross-activate the epidermal growth factor receptor, resulting in a higher activity level of intracellular EGFR cell signaling, resulting in increased cell differentiation and proliferation.[25] Figure 2.4 overlays a small summary of potential COX-2-mediated changes in various cancers. The numerous impacts of COX-2 overexpression underscore the validity and potential of the enzyme as a therapeutic target for the treatment of cancer.

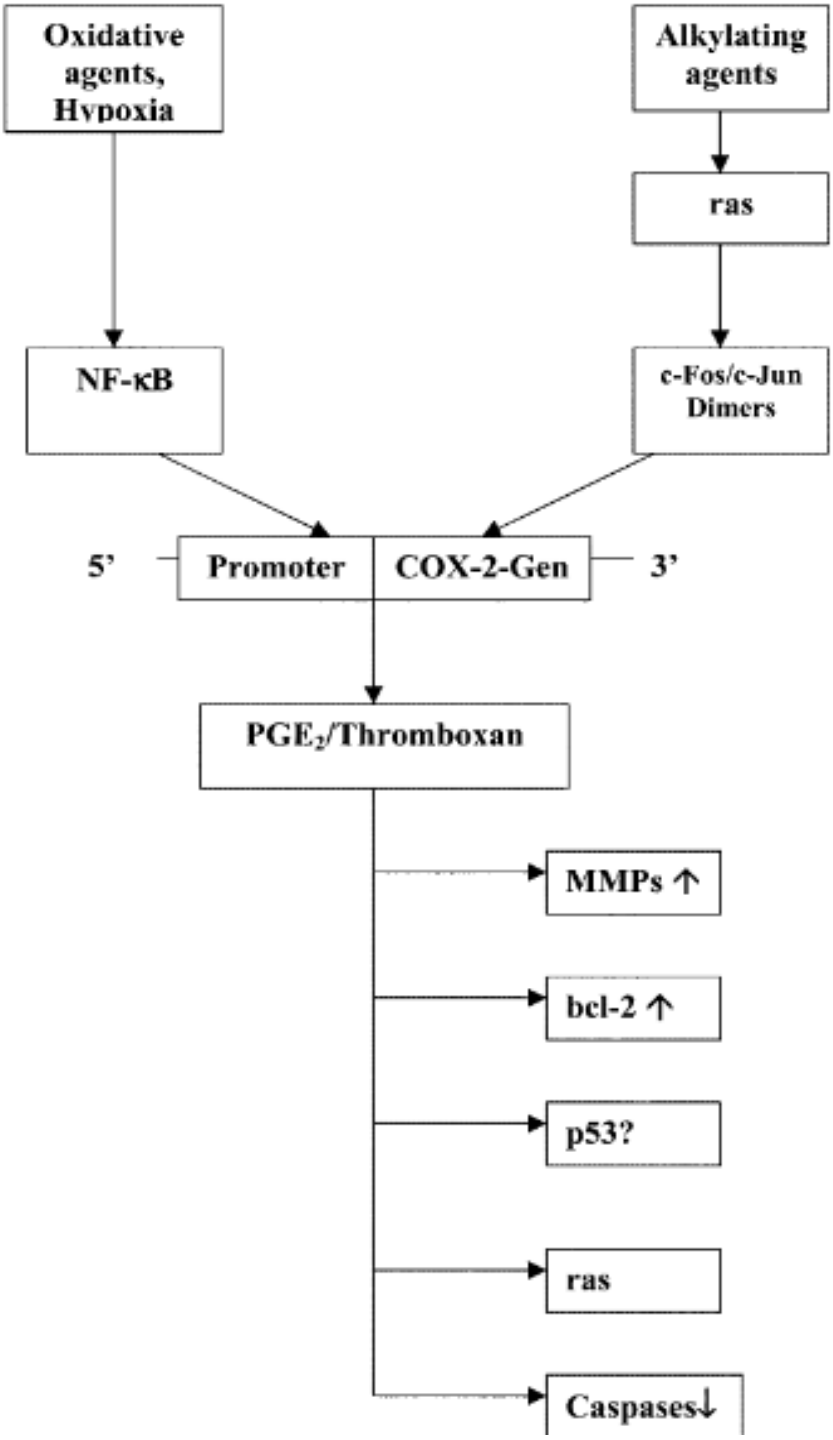

Figure 2.4 – COX-2 activation and potential downstream effects of eicosanoid synthesis in cancer. COX-2 activation can occur via numerous stimuli, which ultimately activate NF-κB and or AP-1 (c-Fos/c-Jun dimers) to transcribe the gene. Downstream effects of PGE_2 and Thromboxanes result in increases in MMPs, Bcl-2, changes in ras-mediated cell signaling, decreases in caspase expression, and possible p53 induction. Abbreviations: NF-κB; Nuclear Factor kappa-light-chain-enhancer of activated B cells; PGE_2; Prostaglandin E_2; MMP; Matrix metalloproteinase; Bcl-2; B-cell lymphoma 2. Figure adapted from Dempke, Wolfram *et al.*[17]

The potential for COX inhibition has led to the development of numerous NSAIDs. Figure 2.5 shows a table of more traditional NSAIDs that have been developed for COX inhibition.[26] Many of these NSAIDs can be broken up into classes based on chemical structure (Fig. 2.5). More recently, newer NSAIDs are classified by mechanism of action. COX-2 specific inhibitors, known as Coxibs, have been a large focus for drug discovery and research due to the desire to improve pain relief while sparing constitutive COX-1 prostanoid production in the gastrointestinal mucosa.[26] Figure 2.6 illustrates the current members of the Coxib family of NSAIDs. The molecular basis for Coxib COX-2 selectivity comes in the form of two criteria: two aromatic rings attached to a heterocycle or carbocycle, and a sulfonamide or sulfone group substituted on the para position of one ring.[27] These functional groups and overall molecular structure were designed on the basis of amino acid differences between COX-1 and COX-2. The latter has a larger active site, which allows for the use of bulky substituents in order to spare the COX-1 isoform by prevention of entry.[28] Firocoxib has been approved for veterinary use. As previously described, it has high clinical efficacy with 350-430 fold selectivity for COX-2 over COX-1. In a pharmacokinetics study performed in horses, Firocoxib was found to have other beneficial properties. The drug has a 30 hour half-life and allows for once-a-day dosing, which is more beneficial for patients.[29] Up to 97% of administered Firocoxib in horses was bound to plasma protein, which aids in biodistribution. Additionally, Firocoxib is highly lipophilic, which aids in its competition for the COX-2 active site against arachidonic acid. The distribution is high for Firocoxib; it has been found to enter even the synovial fluid. The main form of metabolism is hepatic, which involves dealkylation and gluconoridation of the parent compound (Figure 2.7). These metabolites are highly ineffective COX-2 inhibitors that facilitate their own removal from the body via creation of more polar compounds through gluconoridation.[30] Firocoxib excretion is mainly renal, with an average of 68% accounted for in urine. The pharmacokinetic profile of Firocoxib suggests its use for COX-2 inhibition in cancer. In combination with the chemotherapeutic drug cisplatin, Firocoxib improves the remission rate of TCC in canines by 44%, compared to cisplatin alone.[4]

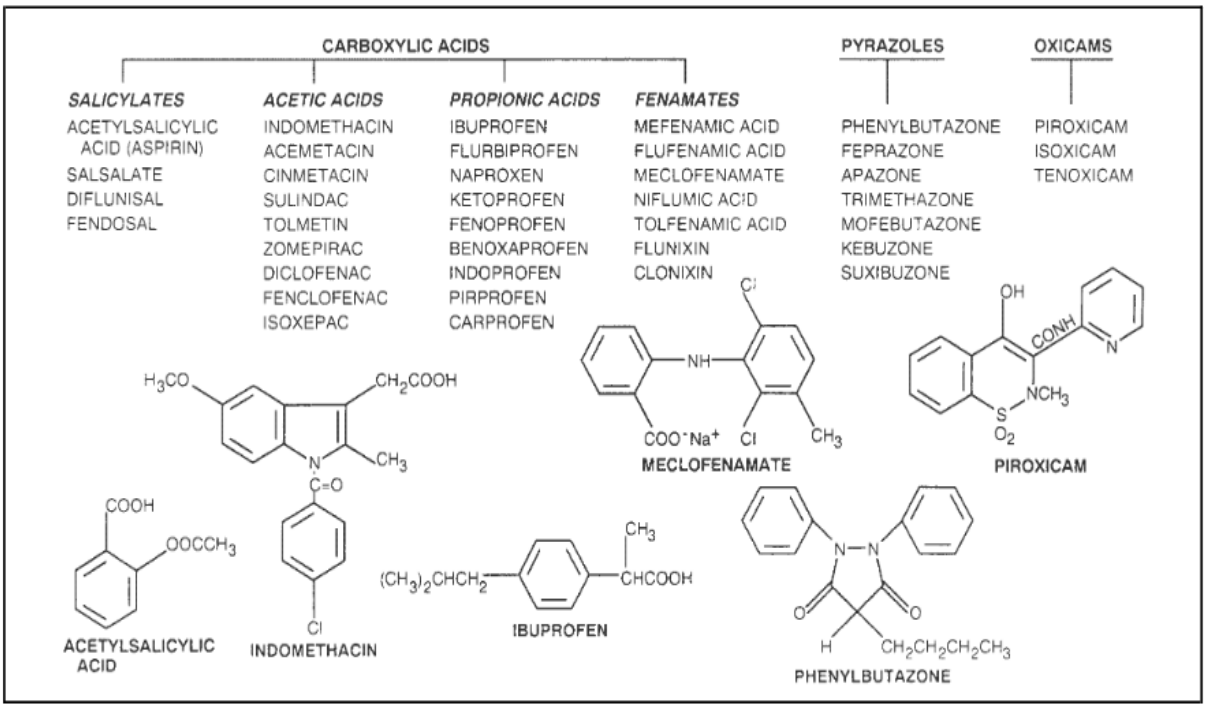

Figure 2.5 – Table of traditional NSAIDs. Many of the typical NSAIDs used are categorized based on chemical structure. Beginning with the salicylates and the development of aspirin, numerous categories of NSAIDs have been developed. Figure adapted from Taketo, Mokoto *et al.*[24]

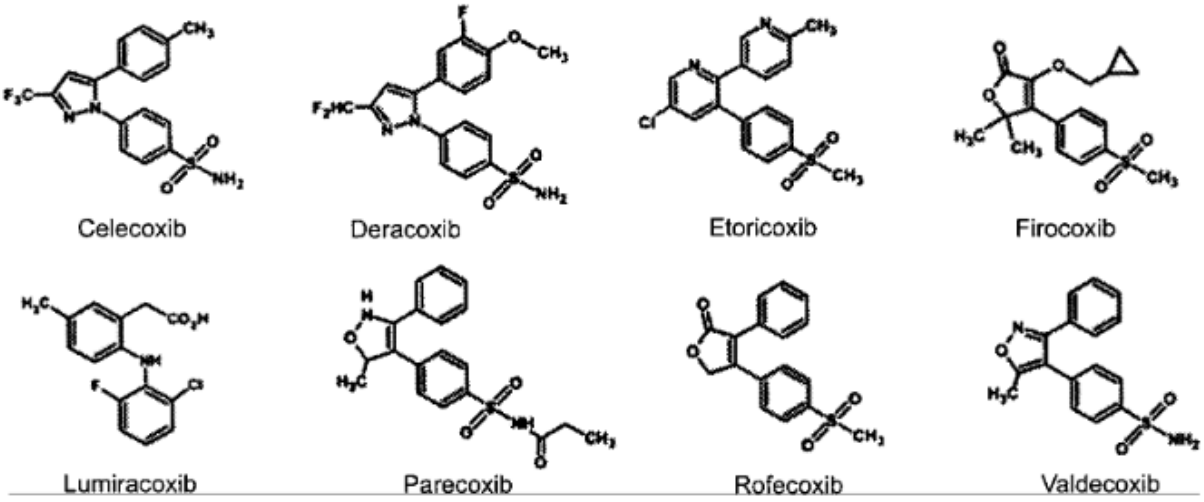

Figure 2.6 – Biochemical structure of the Coxibs. The COX-2 specific NSAIDs, known as the coxibs, are shown above. Rofecoxib (Vioxx) and celecoxib (Celebrex) are the most notorious due to their increased risk for cardiovascular side effects. Firocoxib is currently approved for veterinary use in dogs and horses. Figure adapted from Bergh, Mary Sarah *et al.*[26]

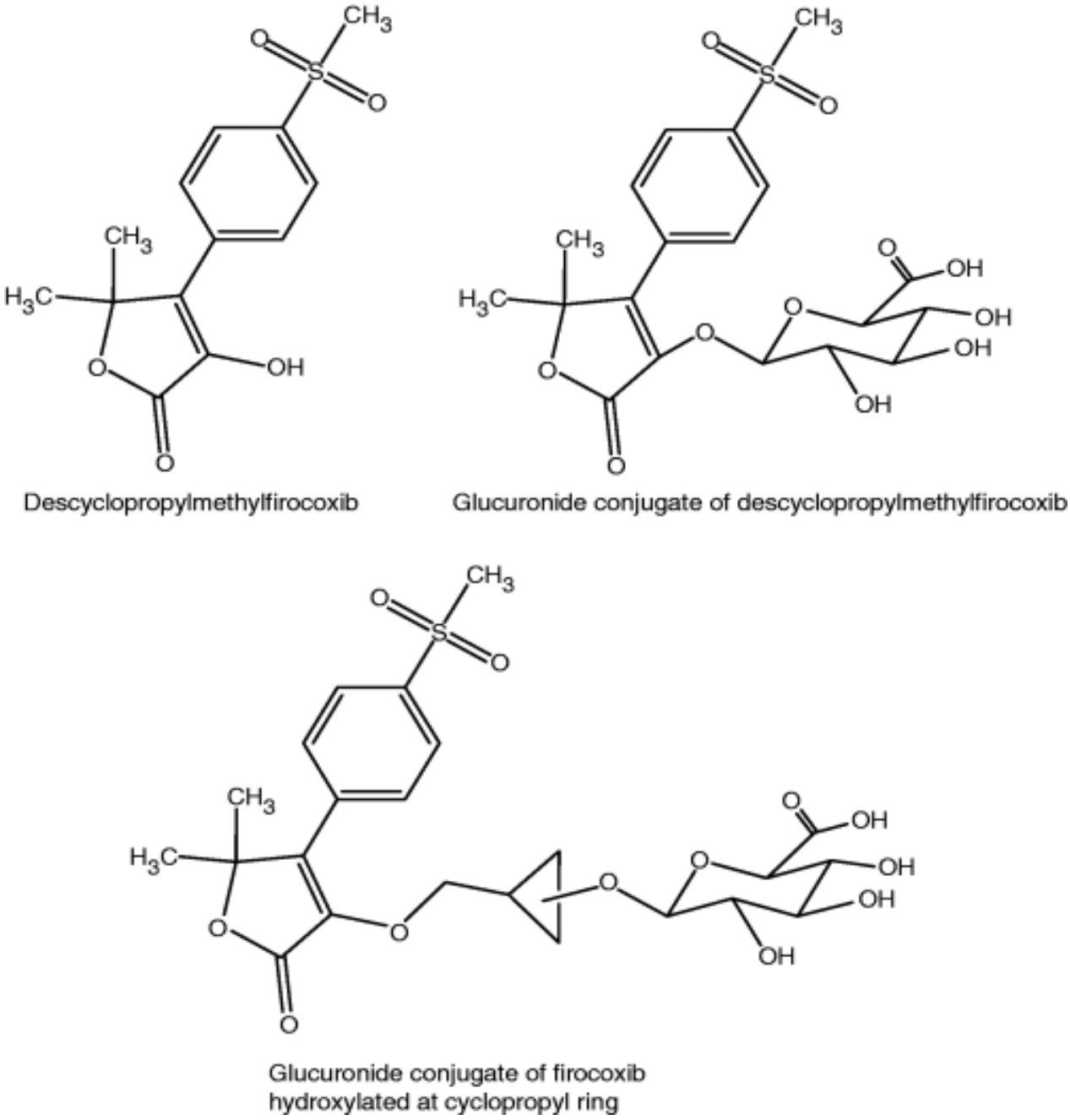

Figure 2.7 – Biochemical structures of major Firocoxib metabolites in horse. There are three major metabolites of Firocoxib formed in the liver. Descyclopropylmethylfirocoxib represents the dealkylated metabolite, which is subsequently gluconoridated. The cyclopropyl ring can also undergo gluconoridation during metabolism. Figure adapted from Kvaternick, V *et al*.[27]

Even with promising therapeutic targets for treatment, the heterogeneity of responses from cancer cells presents another obstacle to overcome. The administration of anticancer drugs in a patient can be complicated by a variety of factors, including drug metabolism, bioavailability, dosage, tumor vascularization, among others.[31] Perhaps the most confounding factor of cancer treatment lies within the genetic makeup and activity of the cancer. Within one tumor type, multiple genotypes can potentially exist as a result of accumulated mutations, epigenetic alterations, and or multidrug resistance proteins (efflux pumps).[32] Some of these epigenetic modifications can result in the modification or removal of a drug target entirely, which confers resistance in many cases. Each type of cancer can express a different selection of drug-resistance genes intrinsically, making treatment options much more limited (Figure 2.8). In the absence of any inherited resistance, treatment with anticancer drugs can result in the selection and overgrowth of treatment-resistant cells.

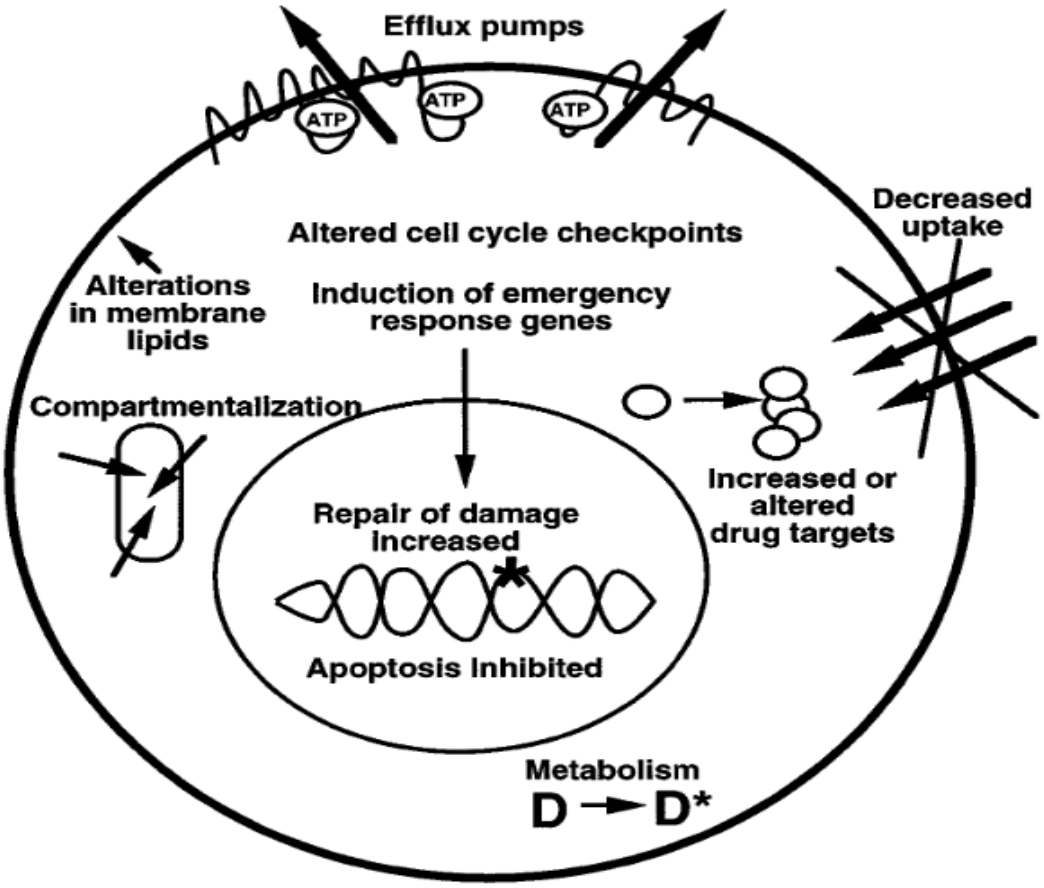

Figure 2.8 – Mechanistic summary of cancer drug resistance. All cancers have various mechanisms of resistance to treatment. Many anticancer drugs are removed from the cancer cells via efflux pumps or sequestered inside the cell. Cancer cells can also limit their uptake of drug or alter the production of the drug targets. Cancer cells can often metabolize drugs and prevent their cytotoxic effects from taking hold. Figure adapted from Gottesman, Michael M.[30]

In order to further understand the role that COX-2 plays in canine TCC, we will investigate the effects of Firocoxib *in vitro*. We will investigate the effects of COX-2 inhibition on PGE_2 concentration, oxidative stress, angiogenesis, cell metabolism and proliferation, *ptgs-2* expression, and the canine TCC proteome. This will help to elucidate the molecular effects of NSAID treatment through COX-dependent and COX-independent mechanisms. We hypothesize that PGE_2 concentration, expression of angiogenic factors, and cell proliferation will decrease. We wish to investigate any effects that Firocoxib may have on oxidative stress to characterize a potential COX-independent mechanism of action. Changes in the canine TCC proteome may occur with Firocoxib treatment, which warrants examination.

3. Experimental Design and Methodology

3.1 – Experimental Design

In order to identify candidate bladder cancer cells for COX-2 inhibition, COX-2 expression must be confirmed in comparison to normal bladder epithelial cells through PCR. For those cells that do express COX-2, treatment with Firocoxib was followed. Mass spectrometry was carried out to identify any changes in canine TCC at the protein level after NSAID treatment. Cell viability assays were performed with Firocoxib in order to identify any direct anti-proliferative effects that NSAID treatment alone may have. Mutations in the active site of the enzyme were investigated as a potential form of NSAID resistance. Immunoblotting was performed to detect the presence of COX-2 protein. Evaluation of PGE_2 concentration was carried out via enzyme immunoassay. Quantification of reactive oxygen species generation was carried out through an intracellular reactive oxygen species assay. The potential angiogenic effects perpetuated through COX-2-mediated signaling, expression of VEGF and its receptor isoforms was investigated and quantified.

3.2 – Methodology

Cell culture and treatment. Five canine TCC cell lines were a kind gift of Dr. Deborah W. Knapp from Purdue University (Orig, IN, AXA, SH, NK). Canine TCC was grown in equal concentrations of DMEM/F12 and supplemented with 100 µg/mL Streptomycin, 100 units/mL Penicillin, 50 µg/mL Gentamicin, and 2 mM of GlutaMAX™ (L-alanyl-L-glutamine, Life Technologies, 35050-061). Cell lines were incubated at 37°C with 5% CO_2 and grown to confluence. Tissue samples were obtained from the OSU College of Veterinary Medicine Biodepository. Cells were treated with Firocoxib at 0.5, 1, 5, and 10 µM respectively. DMSO was used as a vehicle control treatment.

MTT Cell Proliferation Assay. Cell proliferation assays were conducted using MTS reagent (Promega). In 96-well tissue culture plates, 10,000 cells from Orig or NK cell lines were plated and grown to confluence. Cells were starved for 24 hours, and then treated with Firocoxib in 100 µL serum-free media for 24 hours. For each well containing cells, 10 µL of MTS reagent was added in 100 µL of total media. Cells were incubated for 4 hours with reagent, and well absorbance was read on a microplate spectrophotometer (Thermo Scientific Multiskan™ GO) at 490 nm.

Intraceullar Reactive Oxygen Species Assay. Reactive oxygen species quantitation was performed using an Intracellular ROS Assay kit (Cell Biolabs, Inc., STA-342). In 96-well tissue culture plates, 10,000 cells from Orig or NK cell lines were plated and grown to confluence. Cells were then starved for 24 hours. After starvation, cells were treated with 100 µL of a 1X DCFH-DA/media solution and incubated for one hour. After the incubation step, cells were treated with Firocoxib in new serum-free media for 24 hours. Cells were then lysed after Firocoxib treatment. From this lysate, 100 µL was transferred to a black 96-well plate

suitable for fluorescence measurement. Fluorescence measurement was read at 485 nm (excitation) and 528 nm (emission) using a fluorescent plate reader (BioTek FLx800™).

PGE_2 Enzyme Immunoassay. Quantitation of PGE_2 was conducted with a high-sensitivity enzyme immunoassay kit (Arbor Assays, K018-HX1). Protein from TCC cell lysate was loaded in duplicate (25 µL per well) on a coated 96-well plate. Conjugate and detection antibodies were added to appropriate wells. The plate was sealed and shaken at room temperature for 2 hours. Wells were washed, treated with TMB substrate, and incubated for 30 minutes at room temperature without shaking. Stop solution was added and optical density was read at 450 nm using a microplate spectrophotometer (Thermo Scientific Multiskan™ GO) .

Western Blotting. NK or Orig cells were grown to confluence, starved for 24 hours, and collected in RIPA buffer after 24 hours of Firocoxib treatment. Protein from cell lysates was quantified using a bicinchoninic acid assay (BCA™ Protein Assay Kit, Thermo Scientific, #23225). A microplate spectrophotometer (Thermo Scientific Multiskan™ GO) was used to read protein lysates at 562 nm. A primary COX-2 antibody (Novus, H00005743-B01P, mouse anti-human) was used to probe cell lysates. The secondary antibody used to detect COX-2 (Novus, NB7539) is goat anti-mouse. HRP bound to the secondary antibodies was detected using chemiluminescent reagent. Primary tubulin antibody (Santa Cruz Biotechnology, J0109) was used to assess protein loading. The secondary antibody used to detect tubulin was goat anti-rabbit (Santa Cruz Biotechnology, C2112) and was detected in the above manner.

PCR and Real-time RT-PCR. RNA was collected using TRIzol® (Life Technologies) and later mixed with chloroform for extraction. The mixture was centrifuged, and the top phase of the supernatant was removed and mixed with isopropanol. Samples were mixed thoroughly and centrifuged. The resulting RNA pellet was washed with 250 µL of 70% ethanol and air dried. The RNA pellet was re-suspended in water and then mixed with 3M sodium acetate, 0.05-1.0 µg/µL of glycogen, and 80 µL of 100% ethanol. This mixture was incubated overnight at -80°C. The re-precipitated RNA was then centrifuged, washed with 250 µL of 70% ethanol, air dried, and re-suspended in water. Tissue samples were processed in a similar manner. Per sample, 1 µg of RNA was used in a reverse transcription reaction to create cDNA. This reaction was carried out using a High Capacity cDNA Reverse Transcription Kit (Applied Biosystems, Catalog # 4368814). Total reaction volume was 20 µL. To each completed reaction, 100 µL of water was added.

Specific primers were designed to amplify a portion of the coding region of *ptgs-1*, *ptgs-2*, *prdx-1*, *prdx-5*, *prdx-6*, *sod-1*, *vegfa*, *vegfr1* and *vegfr2*. All primers were designed to span an intron. All PCR reactions used a 10 µL total volume. PCR reactions were loaded into either a Dynalon DCL25 DyNAcycler DCL Thermal Cycler, or a Techne TC-512 Thermal Cycler. The PCR reaction cycle used is as follows: One 5-minute 94°C initial denaturation step, followed by 40 cycles of a 30-second 94°C denaturation step, a 30-second, primer-optimized annealing step (57, 59, 61, or 63 °C), and a 30-second 68°C extension step. RT-PCR was

carried out in a similar manner with a 70°C extension step. PCR was conducted using Platinum® *Taq* DNA Polymerase High Fidelity and analyzed by agarose gel electrophoresis on 2% agarose gels. Quantitative RT-PCR was executed with Power SYBR™ using the StepOnePlus Real-Time PCR system (Life Technologies). Relative target gene expression was calculated by the $2^{-\Delta\Delta CT}$ method in relation to their endogenous expression of *ywhaz* and to a vehicle control. PCR primers and their reaction conditions are displayed in Figure 3.2.1.

Primer	Sequence (5' – 3')	Annealing Temperature in °C	Expected Product Size
PRDX-1 F1	GGTTCAGGCCTTCCAGTTTA	59	130
PRDX-1 R2	AGGCGCTCACTTCTGCTTAG		
PRDX-5 F1	GTCTGCAGCACAGGCAGTGT	59	198
PRDX-5 R2	CTTGCCCTTGAACAGCTCTG		
PRDX-6 F1	GCAAAGCTGGCACCAGAAT	59	115
PRDX-6 R2	CCTGCCCATTGTAGGCATT		
PTGS-1 F1	GCATCGCCATGGAGTTCAA	57	102 or 213
PTGS-1 R2	CGTGCAGGACATGGTGGTC		
PTGS-2 F3	TTCCAGACGAGCAGGCTAAT	59	112
PTGS-2 R4	GCAGCTCTGGGTCAAACTTC		
SOD-1 F1	GTGGCCATTGTGTCCATAGA	59	163
SOD-1 R2	CACCACAAGCCAAACGACT		
VEGFA F1	GGCAGGAGGAGAGCACAA	61	94
VEGFA R2	GATGTCCACCAGGGTCTCAA		
VEGFR1 F1	GGCTCAGGCAAACCACAC	63	190
VEGFR1 R2	CCGGCAGGGGATGACGAT		
VEGFR2 F1	GGAAGAGGAAGTGTGTGACCCC	63	181
VEGFR2 R2	GACCATACCACTGTCCGTCTGG		
YWHAZ F1	AGCCTGCTCTCTTGCAAAGAC	59	137
YWHAZ R2	GGGTATCCGATGTCCACAATG		

Figure 3.2.1 – PCR primers and reaction conditions. Abbreviations: PRDX = Peroxiredoxin, PTGS = Prostaglandin Synthase, SOD-1 = Superoxide Dismutase, VEGFA = Vascular endothelial growth factor A, VEGFR1 = Vascular endothelial growth factor receptor 1, VEGFR2 = Vascular endothelial growth factor receptor 2, YWHAZ = Tyrosine 3-monooxygenase/tryptophan 5-monooxygenase activation protein zeta

Mass Spectrometry. Once cells reached confluency and were starved for 24 hours, protein lysates were collected in RIPA buffer containing protease and phosphatase inhibitors with a cell scraper. Lysates were quantified using the previously-described bicinchoninic acid assay, centrifuged to remove debris, and the supernatant was digested with trypsin. All samples were processed in the Synapt G2 using LC-MS/MS, as well as a hybrid mass spectrometer (LTQ FT). All LC-MS/MS samples were analyzed using Mascot (Matrix Science, London, UK; version 2.3.0) and X! Tandem (The GPM, thegpm.org; version CYCLONE (2010.12.01.1)). Mascot was set up to search the ABRF_swissprot_human database (unknown version, 69351 entries) assuming the digestion enzyme trypsin. Scaffold (version Scaffold_4.2.1, Proteome Software Inc., Portland, OR) was used to validate MS/MS based peptide and protein identifications. Peptide identifications were accepted if they could be established at greater than 95.0% probability by the Scaffold Local FDR algorithm. Protein identifications were accepted if they could be established at greater than 95.0% probability and contained at least 2 identified peptides.

4. Results

The intent of our study is to elucidate the effects of Firocoxib on canine TCC cells *in vitro*, as its use *in vivo*, in combination with chemotherapeutics, yields improved outcomes through direct and or systemic effects. We first evaluate the cyclooxygenase expression profile of our canine TCC cell lines, three normal bladders, and an inflamed bladder. Constitutive *ptgs-1* expression is present in normal bladders and TCC cell lines (Figure 4.1 – A). In contrast, *ptgs-2* expression is present in low levels in normal bladder epithelia, while Orig and NK express *ptgs-2* to a greater degree (Figure 4.1 – B). Relative to normal bladder epithelia, TCC cell lines exhibit a 15-20 fold increase in *ptgs-2* expression (Figure 4.1 – C). Additionally, most coded primary tissue samples also show elevated *ptgs-2* expression to a lesser degree. COX-2 immunoblotting shows the presence of the protein in lysate from Firocoxib-treated Orig cells (Figure 4.1 – D).

From Firocoxib-treated protein lysate, we quantify PGE_2 concentration to gauge the efficacy of COX-2 inhibition. Across all concentrations, PGE_2 concentration in Orig cells strikingly decreases relative to DMSO-treated vehicle controls (Figure 4.2 – A). Levels of PGE_2 production are as high as 3.5 ng/mL (Cell line Orig) and 17.55 ng/mL (Cell line NK) in vehicle controls, which indicates high basal COX-2 activity. This correlates with the overexpression of *ptgs-2* previously seen.

We also examine the production of reactive oxygen species (ROS) induced by Firocoxib treatment. With Firocoxib-treated Orig cells, ROS production (given in Relative Fluorescence Units [RFU]) increased at 0.5 μM and 1 μM doses (Figure 4.3-A) In NK cells, RFU significantly decreases at the 1 μM and 5 μM doses (Figure 4.3-B). We examined any effect of Firocoxib treatment on gene expression of enzymes that eliminate ROS (*prdx 1, prdx 5, prdx 6, sod-1*). No significant change in any gene expression was seen for these enzymes in Orig cells for all drug concentrations (Figure 4.4 – B,C).

We consider the effects of COX-2 inhibition on expression of *ptgs-2* and angiogenic factors (*vegfa, vegfr1*). Paradoxically, higher doses of Firocoxib (10 μM and 5 μM) induce a 4-fold increase in *vegfr1* expression (Figure 4.4 – A). To assess cell viability with NSAID treatment, we used a MTT colorimetric assay. No significant changes in the proliferative index were observed using Firocoxib in Orig or NK cells (Figure 4.5 – A, B). In order to examine the collective effect of Firocoxib treatment on the TCC proteome, we performed analysis using LC/MS-MS on Firocoxib-treated Orig cell protein lysates. At a 10 μM dose, seven unique peptides were identified, while only 2 unique peptides were distinguished at a 1 μM dose. (Figure 4.6 – A, B).

4.1 – *ptgs*-1/2 Profile of TCC Cell Lines and Normal Bladder Epithelia

A. **B.**

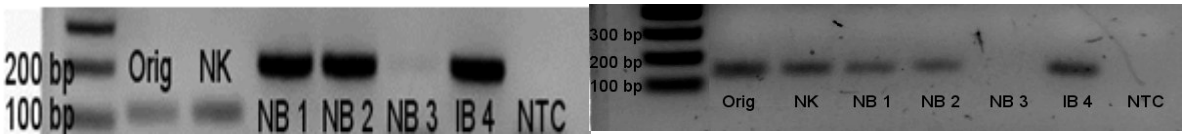

Figure 4.1 – A and 4.1 – B: *ptgs-1* (A) and *ptgs-2* (B) expression through PCR – The expression of *ptgs-1* is shown by Figure 4.1 – A. Lane 1 is a DNA standard ladder. Lanes 2 and 3 show *ptgs-1* expression with a 102 base pair product size. Lanes 4-7 show *ptgs-1* expression with a 212 base pair product size, which indicates a different transcript variant being expressed. Lane 8 represents a no-template control PCR reaction

Expression of *ptgs-2* is shown by Figure 4.1 – B. Lane 1 is a DNA standard ladder. Lanes 2-7 show *ptgs-2* expression for each sample cDNA except NB 3. Lane 8 represents a no-template control PCR reaction.

Abbreviations: Orig = TCC Cell line “Original”, NK = TCC Cell line NK, NB = Normal bladder epithelia, IB = Inflamed bladder, NTC = No template control

C.

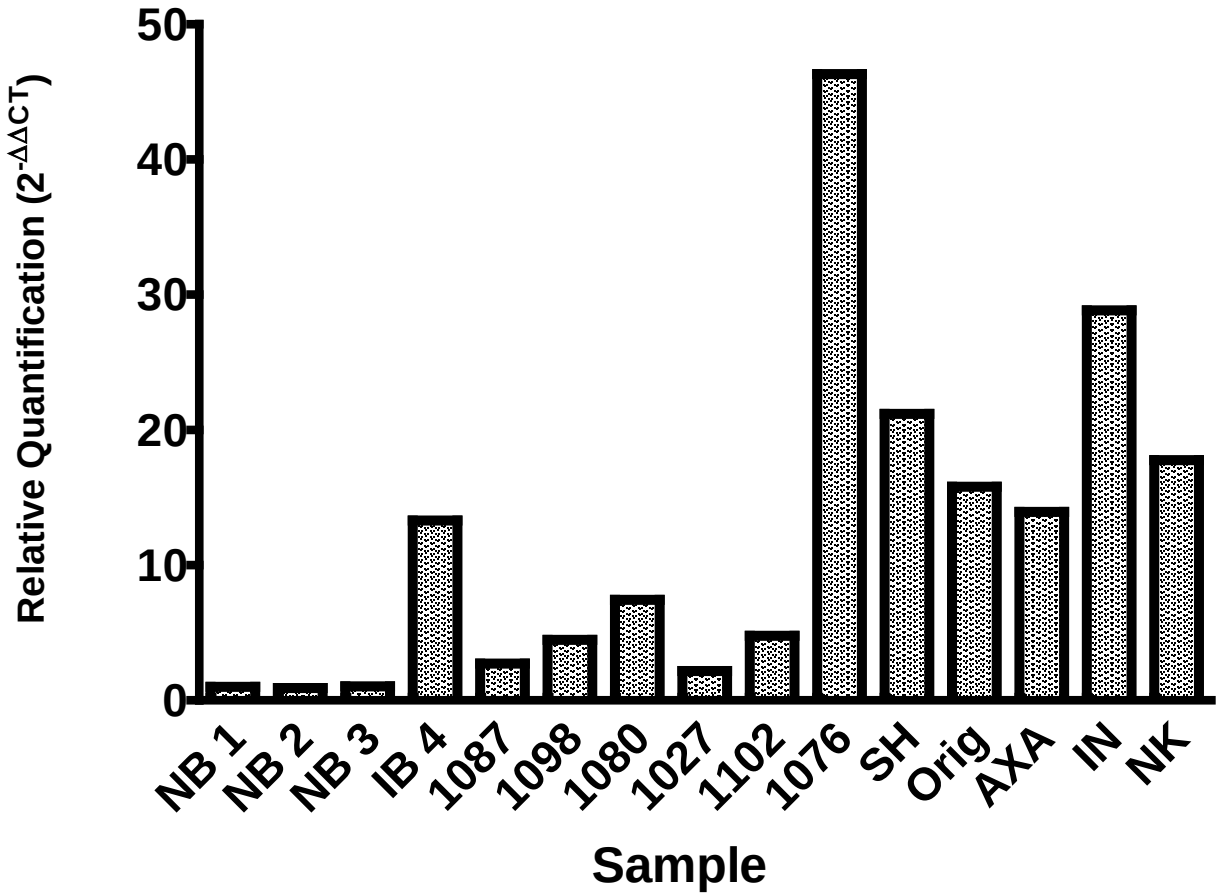

Figure 4.1 – C: Quantification of *ptgs-2* expression relative to normal bladder epithelia – Quantitative RT-PCR analysis of cDNAs from normal bladder epithelia samples, primary TCC tissue samples, and TCC cell lines is shown. Analysis of data through the $2^{-\Delta\Delta CT}$ method provides fold-change values for relative *ptgs-2* expression. Compared to normal bladder epithelia, TCC cell lines exhibit a large 15-20 fold increase in gene expression. Primary tissue samples also display increased expression to a lesser degree.

Abbreviations: NB = Normal bladder epithelia, IB = Inflamed bladder, 1087-1076 = Primary TCC tissue sample VetHosp number, SH-NK = TCC cell lines

D.

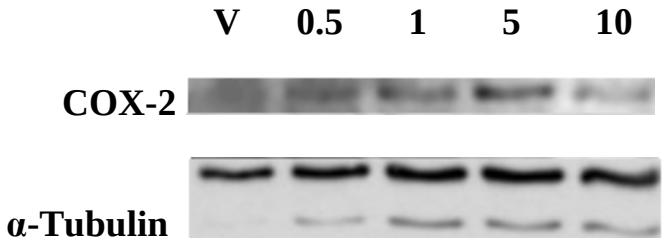

Figure 4.1 – D – Immunoblotting of COX-2 Protein – Western blotting was used to detect COX-2 protein in Firocoxib-treated protein lysates from the Orig cell line. The top row of bands shows the presence of COX-2 protein. The bottom row of bands displays α-tubulin protein used to assess protein loading.

Abbreviations: V = DMSO (dimethylsulfoxide) vehicle control, 0.5 – 10 = concentration of Firocoxib (µM), COX-2 = cyclooxygenase-2 protein, α-tubulin = alpha tubulin protein.

4.2 – Quantification of PGE_2 production after treatment with Firocoxib

A.

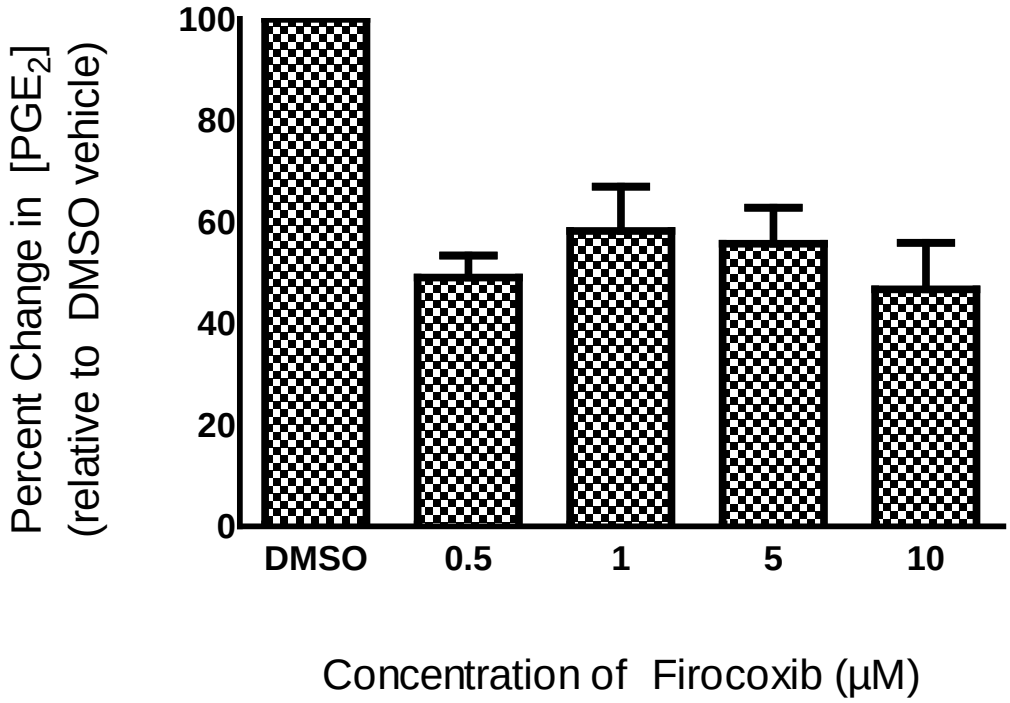

Figure 4.2 – A: Change in PGE_2 concentration relative to DMSO-treated vehicle control – Using a PGE_2 enzyme immunoassay, concentrations of PGE_2 in Firocoxib-treated TCC cell line protein lysates were quantified. Firocoxib treatment at all concentrations result in significant 40-50% decreases in PGE_2 concentration.

Abbreviations: DMSO = Dimethylsulfoxide

B.

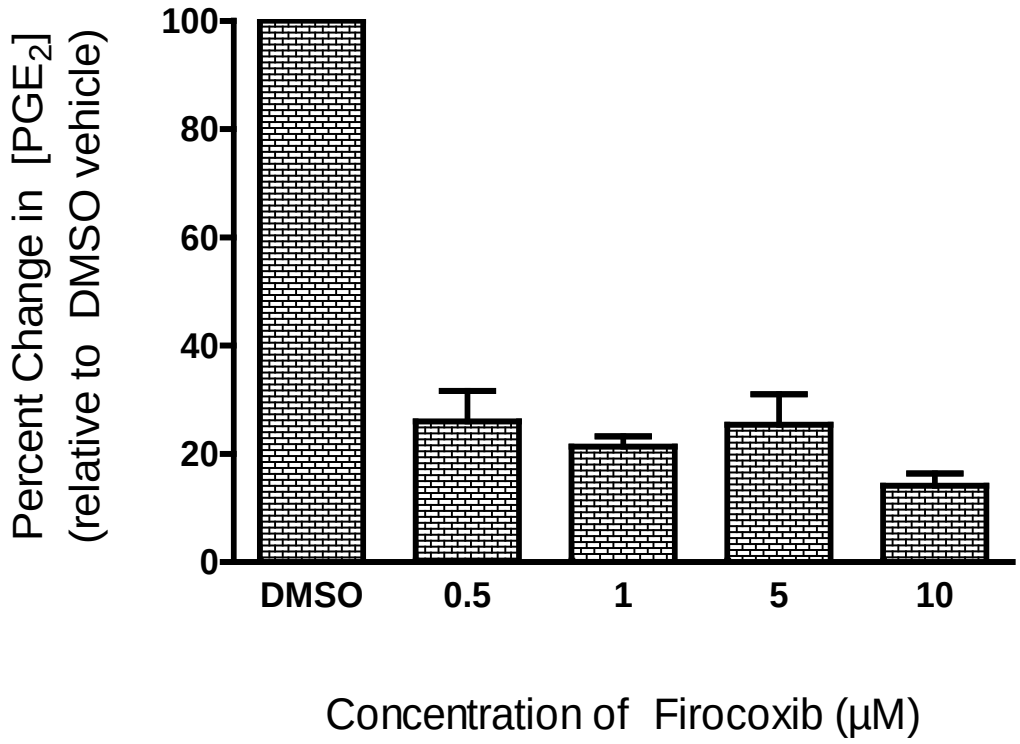

Figure 4.2 – B: Change in PGE_2 concentration relative to DMSO-treated vehicle control – Using a PGE_2 enzyme immunoassay, concentrations of PGE_2 in Firocoxib-treated TCC cell line protein lysates were quantified. Firocoxib treatment at all concentrations result in significant 70-80% decreases in PGE_2 concentration.

Abbreviations: DMSO = Dimethylsulfoxide,

4.3 – Reactive Oxygen Species (ROS) generation after Firocoxib treatment

A.

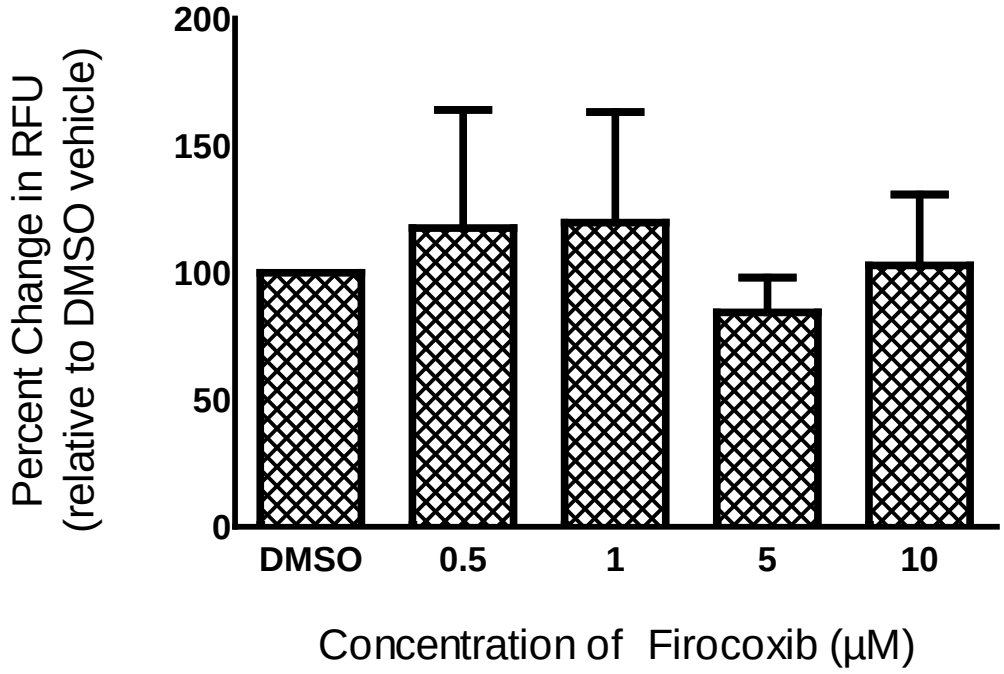

Figure 4.3 – A: Percentage change in RFUs after Firocoxib treatment in Orig cells relative to DMSO-treated vehicle controls – Using an intracellular reactive oxygen species (ROS) assay, ROS levels were quantified in RFU. In TCC Orig cells, increases in RFU were seen at 0.5 and 1 µM doses.

Abbreviations: RFU = Relative Fluorescent Units, DMSO = Dimethylsulfoxide

B.

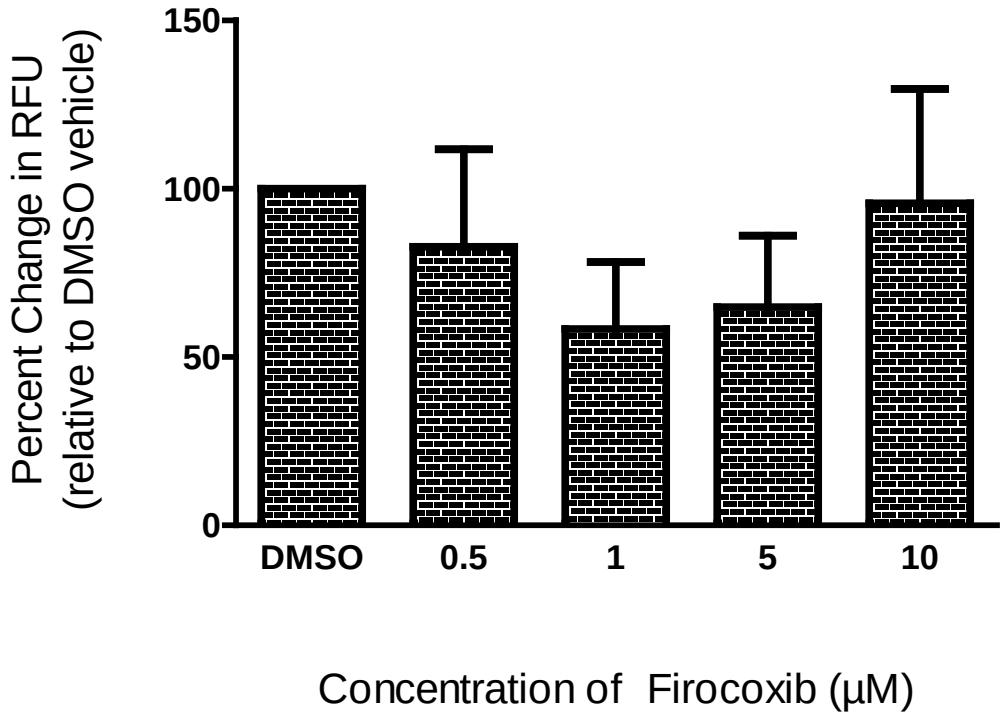

Figure 4.3 – B: Percentage change in RFUs after Firocoxib treatment in NK cells relative to DMSO-treated vehicle controls – Using an intracellular reactive oxygen species (ROS) assay, ROS levels were quantified in RFU. In TCC NK cells, decreases in RFU were seen at 0.5, 1, and 5 µM doses.

Abbreviations: RFU = Relative Fluorescent Units, DMSO = Dimethylsulfoxide

4.4 – qPCR Quantification of gene expression after Firocoxib treatment

A.

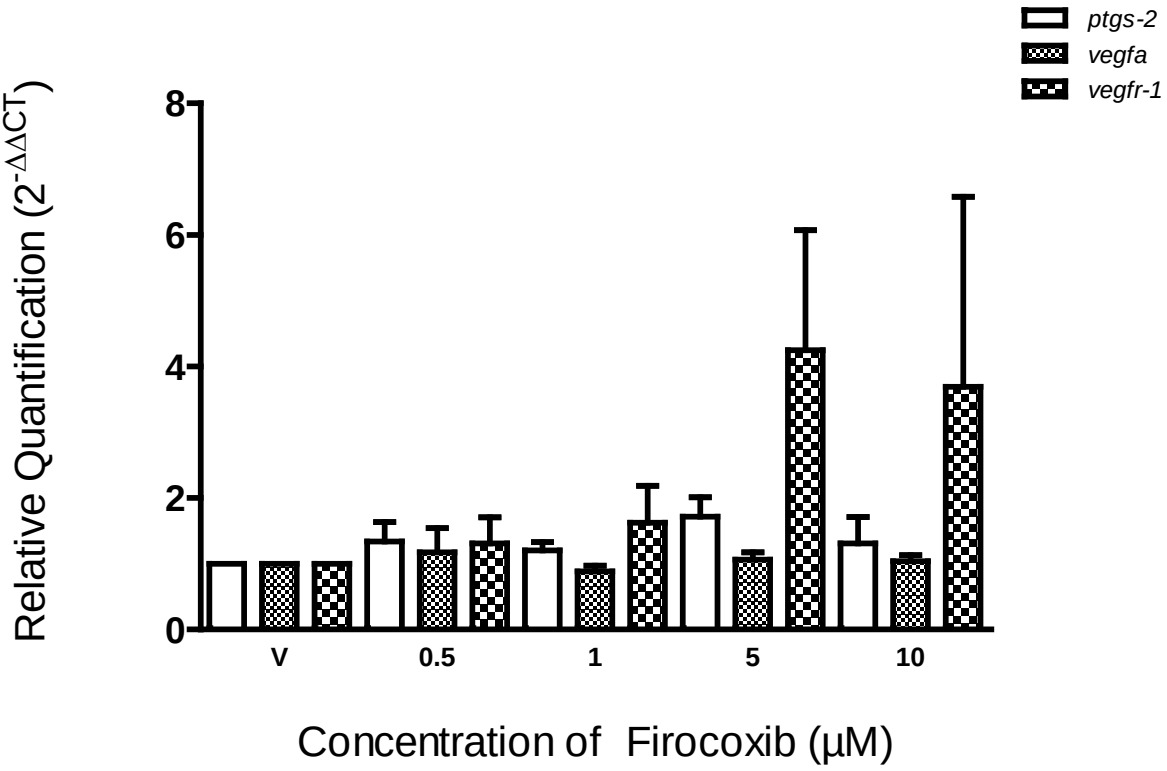

Figure 4.4 – A: Quantification of *ptgs-2, vegfa,* and *vegfr1* expression after Firocoxib treatment – Through RT-PCR, changes in *ptgs*-2, *vegfa*, and *vegfr-1* expression were quantified. At 5 and 10 µM doses, expression of *vegfr-1* increased significantly. No other changes in gene expression at any dose were seen.

Abbreviations: DMSO = Dimethylsulfoxide, *ptgs-2* = cyclooxygenase-2 (prostaglandin synthase), *vegfa* = vascular endothelial growth factor A, *vegfr1* = vascular endothelial growth factor receptor 1

B.

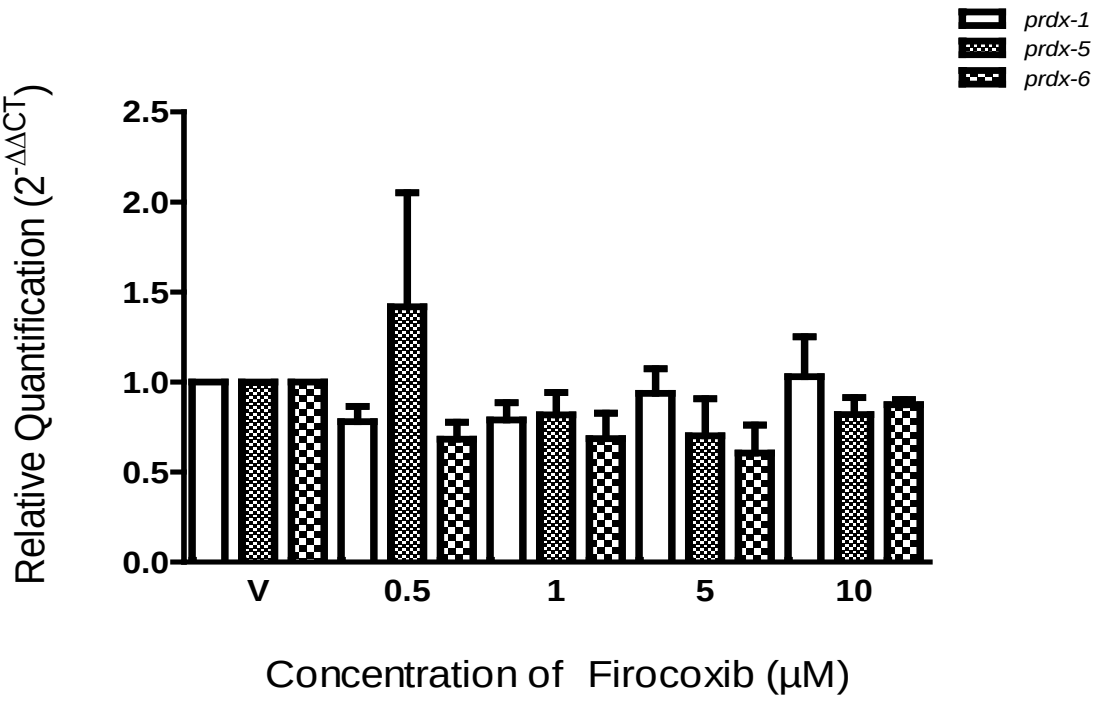

Figure 4.4 – B: Quantification of *prdx-1, prdx-5,* and *prdx-6* expression after Firocoxib treatment – Quantitative RT-PCR was used to investigate the changes of *prdx-1*, *prdx-5*, and *prdx-6* expression. No significant changes for any gene were seen.

Abbreviations: DMSO = Dimethylsulfoxide, *prdx-1* = peroxiredoxin-1, *prdx-5* = peroxiredoxin-5, *prdx-6* = peroxiredoxin-6

C.

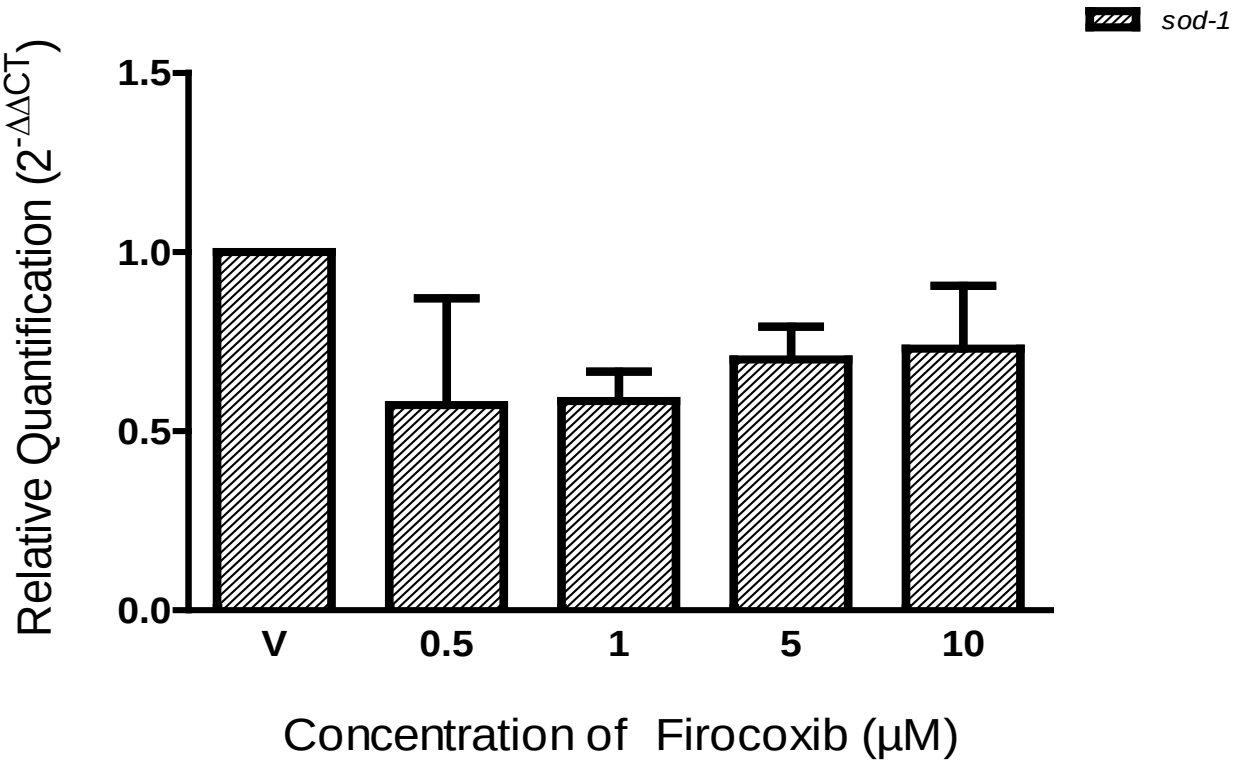

Figure 4.4 – B: Quantification of *sod-1* expression after Firocoxib treatment – Further RT-PCR analysis on *sod-1* gene expression was carried out. No significant changes in gene expression were seen at any dose.

Abbreviations: DMSO = Dimethylsulfoxide, *sod-1* = Superoxide dismutase

4.5 – MTT Cell proliferation Assays

A.

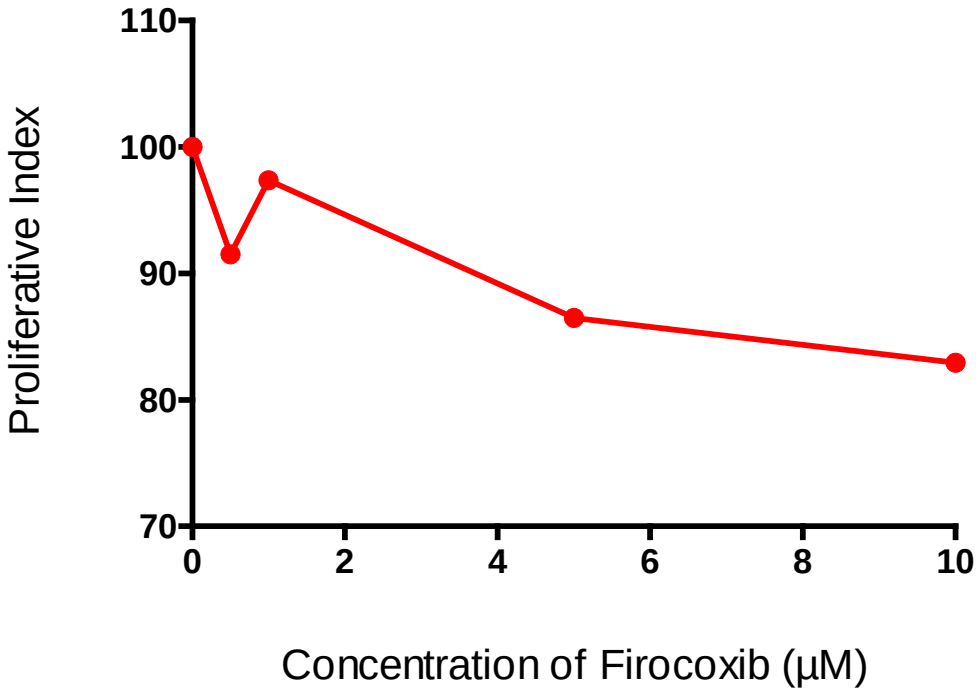

Figure 4.5 – A: Proliferative index of Orig cells after Firocoxib treatment – In a MTT cell proliferation assay, TCC Orig cells were treated with Firocoxib and their proliferative indexes measured. At all concentrations, no significant decrease in the proliferative index was seen. The vehicle control (DMSO) represents a 0 µM concentration of Firocoxib and 100% on the proliferative index.

B.

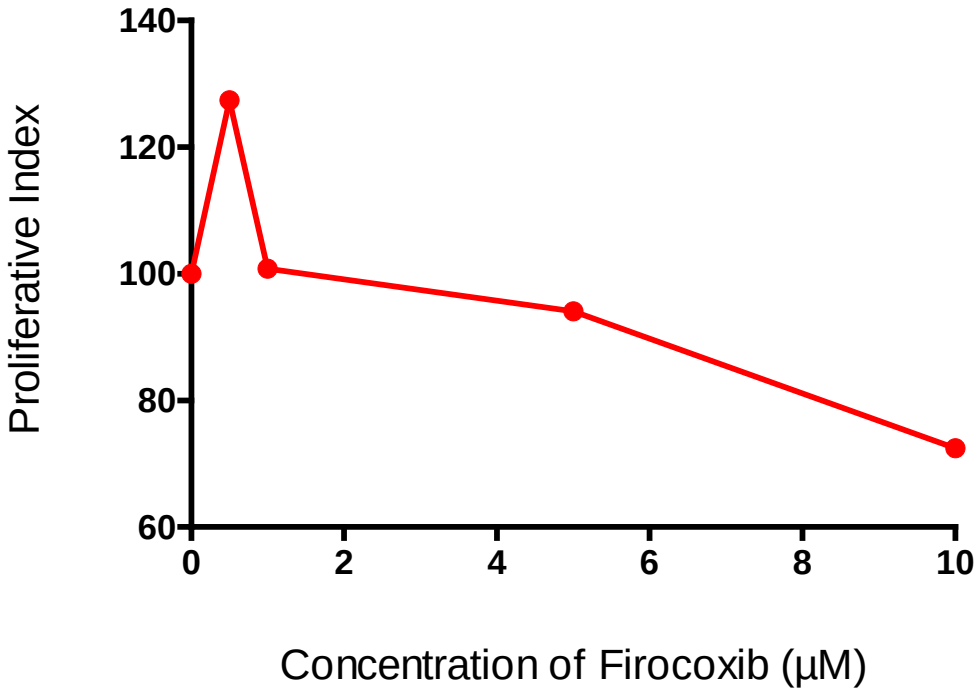

Figure 4.5 – B: Proliferative index of NK cells after Firocoxib treatment – In a MTT cell proliferation assay, TCC NK cells were treated with Firocoxib and their proliferative indexes measured. At all concentrations, no significant decrease in the proliferative index was seen. The vehicle control (DMSO) represents a 0 µM concentration of Firocoxib and 100% on the proliferative index.

4.6 – Evaluation of the TCC proteome post-treatment with Firocoxib

A.

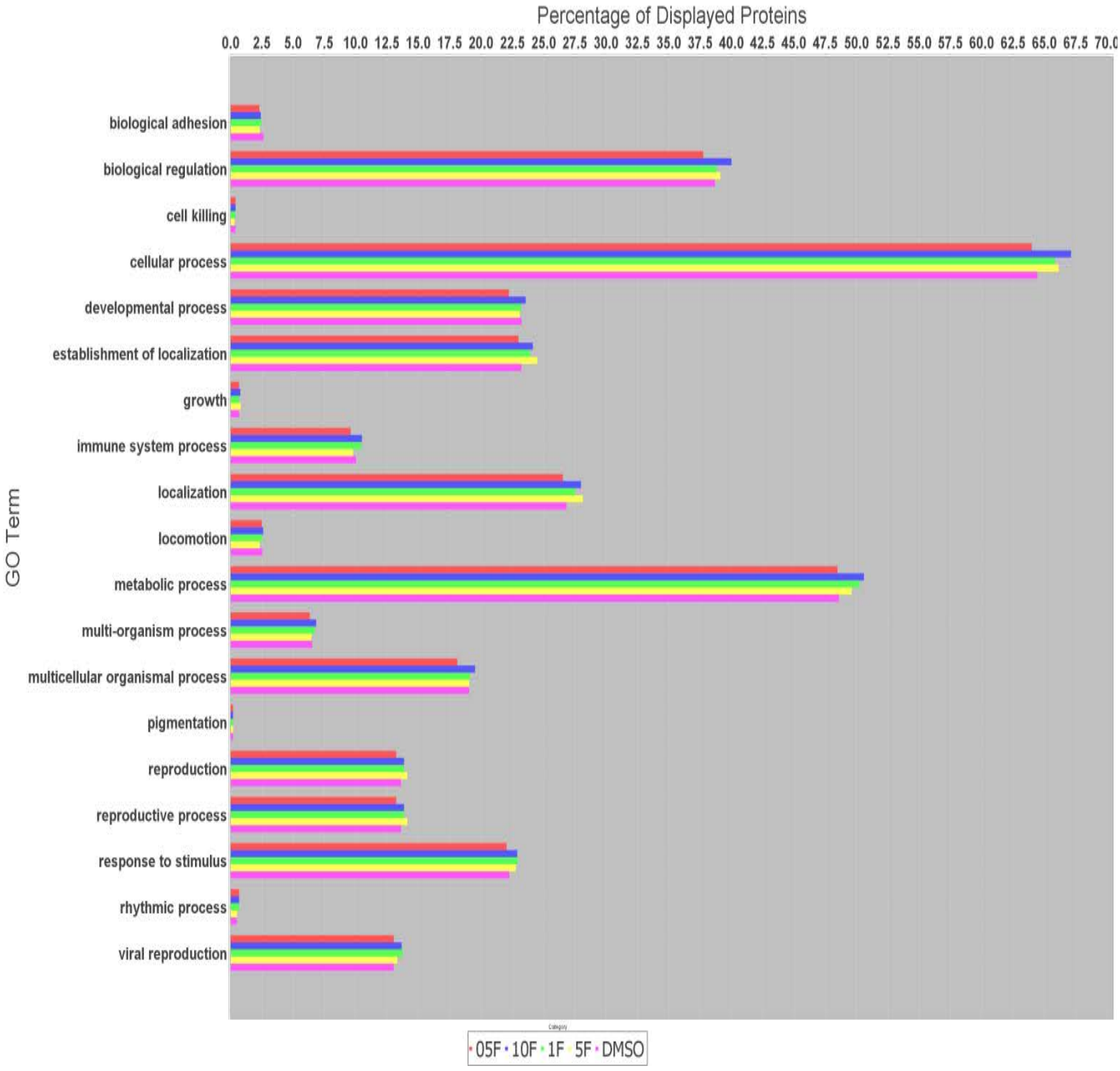

Figure 4.6 – A: Evaluation of the TCC proteome post-treatment: The x-axis represents the percentage of proteins displayed per category in each sample. The y-axis represents categories of proteins based on function. Each color represents a concentration of Firocoxib or the DMSO (dimethylsulfoxide) control.

B.

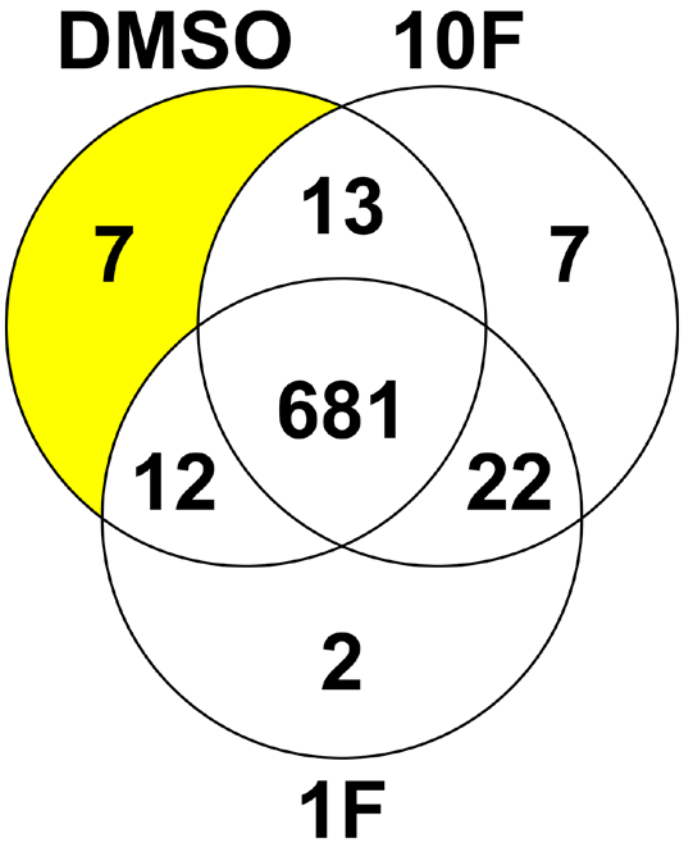

Accession	Protein Name
RD23B_HUMAN	UV excision repair protein RAD23 homolog B OS=Homo sapiens GN=RAD23B PE=1 SV=1
DYH2_HUMAN	Dynein heavy chain 2, axonemal OS=Homo sapiens GN=DNAH2 PE=2 SV=3
GRN_HUMAN	Granulins OS=Homo sapiens GN=GRN PE=1 SV=2
PI42C_HUMAN	Phosphatidylinositol 5-phosphate 4-kinase type-2 gamma OS=Homo sapiens GN=PIP4K2C PE=1 SV=3
DMD_HUMAN	Dystrophin OS=Homo sapiens GN=DMD PE=1 SV=3
RBP56_HUMAN	TATA-binding protein-associated factor 2N OS=Homo sapiens GN=TAF15 PE=1 SV=1
Q5RI18_HUMAN	Heterogeneous nuclear ribonucleoprotein U (Fragment) OS=Homo sapiens GN=HNRNPU PE=2 SV=1

Figure 4.6 – B: Evaluation of the TCC proteome post-treatment: The Venn diagram contains unique proteins for each sample. The overlapping sections represent proteins that are common to each pair of samples, or all three. The DMSO (dimethylsulfoxide) control was compared to a high dose (10 μM) and low dose (1 μM) of Firocoxib. The protein identities above are derived from the unique proteins highlighted in yellow.

C.

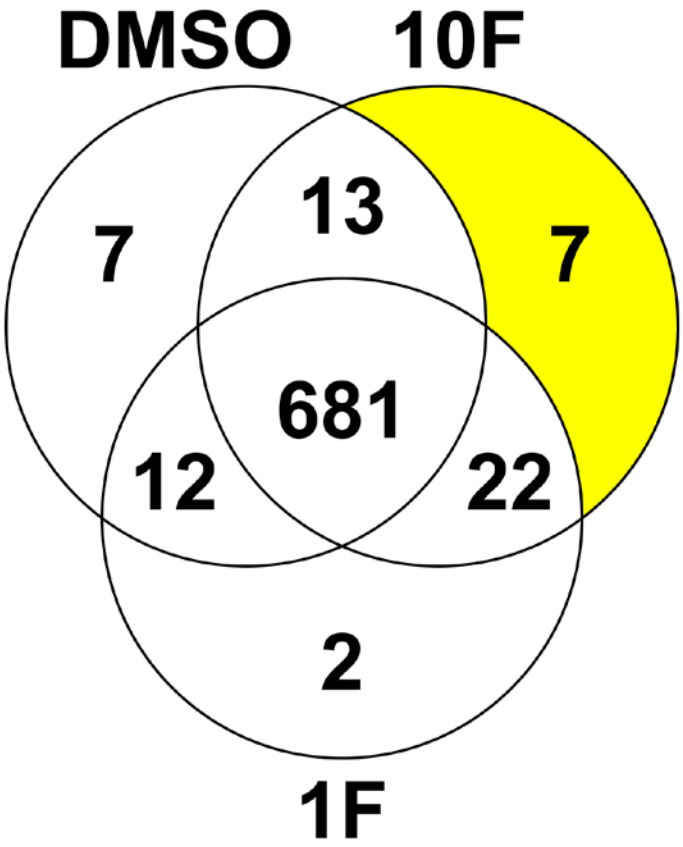

Accession	Protein Name
CASPC_HUMAN	Inactive caspase-12 OS=Homo sapiens GN=CASP12 PE=2 SV=2
AL9A1_HUMAN	4-trimethylaminobutyraldehyde dehydrogenase OS=Homo sapiens GN=ALDH9A1 PE=1 SV=3
PPCE_HUMAN	Prolyl endopeptidase OS=Homo sapiens GN=PREP PE=1 SV=2
IPO8_HUMAN	Importin-8 OS=Homo sapiens GN=IPO8 PE=1 SV=2
RASK_HUMAN	GTPase KRas OS=Homo sapiens GN=KRAS PE=1 SV=1
RB27B_HUMAN	Ras-related protein Rab-27B OS=Homo sapiens GN=RAB27B PE=1 SV=4
CYFP2_HUMAN	Cytoplasmic FMR1-interacting protein 2 OS=Homo sapiens GN=CYFIP2 PE=1 SV=2

Figure 4.6 – C: Evaluation of the TCC proteome post-treatment: The Venn diagram contains unique proteins for each sample. The overlapping sections represent proteins that are common to each pair of samples, or all three. The DMSO (dimethylsulfoxide) control was compared to a high dose (10 μM) and low dose (1 μM) of Firocoxib. The protein identities above are derived from the unique proteins highlighted in yellow.

D.

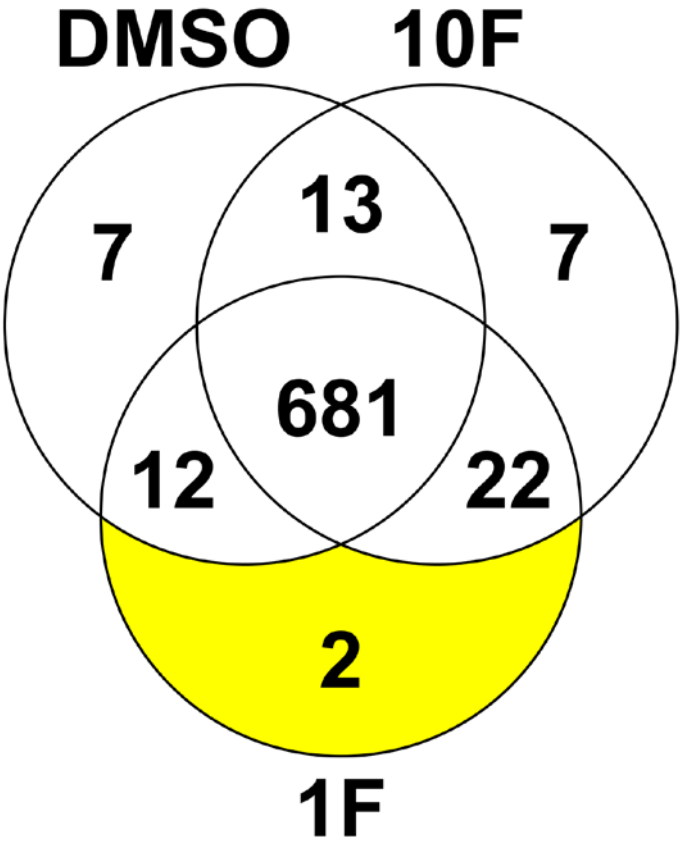

Accession	Protein Name
EHD3_HUMAN	EH domain-containing protein 3 OS=Homo sapiens GN=EHD3 PE=1 SV=2
SCOT1_HUMAN	Succinyl-CoA:3-ketoacid coenzyme A transferase 1, mitochondrial OS=Homo sapiens GN=OXCT1 PE=1 SV=1

Figure 4.6 – D: Evaluation of the TCC proteome post-treatment: The Venn diagram contains unique proteins for each sample. The overlapping sections represent proteins that are common to each pair of samples, or all three. The DMSO (dimethylsulfoxide) control was compared to a high dose (10 μM) and low dose (1 μM) of Firocoxib. The protein identities above are derived from the unique proteins highlighted in yellow.

E.

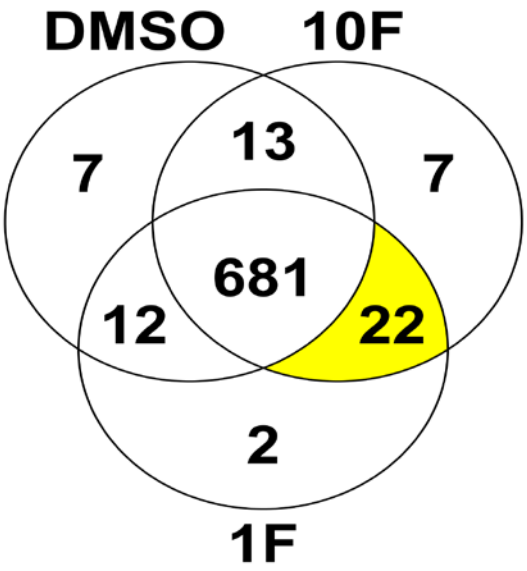

Accession	Protein Name
XPOT_HUMAN	Exportin-T OS=Homo sapiens GN=XPOT PE=1 SV=2
LYPA2_HUMAN	Acyl-protein thioesterase 2 OS=Homo sapiens GN=LYPLA2 PE=1 SV=1
ABCE1_HUMAN	ATP-binding cassette sub-family E member 1 OS=Homo sapiens GN=ABCE1 PE=1 SV=1
MVP_HUMAN	Major vault protein OS=Homo sapiens GN=MVP PE=1 SV=4
SMD2_HUMAN	Small nuclear ribonucleoprotein Sm D2 OS=Homo sapiens GN=SNRPD2 PE=1 SV=1
S22AB_HUMAN	Solute carrier family 22 member 11 OS=Homo sapiens GN=SLC22A11 PE=1 SV=1
J3QRV5_HUMAN	Lethal(2) giant larvae protein homolog 2 OS=Homo sapiens GN=LLGL2 PE=4 SV=1
NDUS1_HUMAN	NADH-ubiquinone oxidoreductase 75 kDa subunit, mitochondrial OS=Homo sapiens GN=NDUFS1 PE=1 SV=3
TRAP1_HUMAN	Heat shock protein 75 kDa, mitochondrial OS=Homo sapiens GN=TRAP1 PE=1 SV=3
FUMH_HUMAN	Fumarate hydratase, mitochondrial OS=Homo sapiens GN=FH PE=1 SV=3
PSMD6_HUMAN	26S proteasome non-ATPase regulatory subunit 6 OS=Homo sapiens GN=PSMD6 PE=1 SV=1
DDX6_HUMAN	Probable ATP-dependent RNA helicase DDX6 OS=Homo sapiens GN=DDX6 PE=1 SV=2
EIF3E_HUMAN	Eukaryotic translation initiation factor 3 subunit E OS=Homo sapiens GN=EIF3E PE=1 SV=1
RAB5C_HUMAN	Ras-related protein Rab-5C OS=Homo sapiens GN=RAB5C PE=1 SV=2
CSK21_HUMAN	Casein kinase II subunit alpha OS=Homo sapiens GN=CSNK2A1 PE=1 SV=1
B7Z972_HUMAN	Protein-L-isoaspartate O-methyltransferase OS=Homo sapiens GN=PCMT1 PE=2 SV=1
CMC2_HUMAN	Calcium-binding mitochondrial carrier protein Aralar2 OS=Homo sapiens GN=SLC25A13 PE=1 SV=2
RAB3D_HUMAN	Ras-related protein Rab-3D OS=Homo sapiens GN=RAB3D PE=1 SV=1
ERMP1_HUMAN	Endoplasmic reticulum metallopeptidase 1 OS=Homo sapiens GN=ERMP1 PE=1 SV=2
AT2A1_HUMAN	Sarcoplasmic/endoplasmic reticulum calcium ATPase 1 OS=Homo sapiens GN=ATP2A1 PE=1 SV=1
GMDS_HUMAN	GDP-mannose 4,6 dehydratase OS=Homo sapiens GN=GMDS PE=1 SV=1
J3QST3_HUMAN	Keratin, type II cytoskeletal 3 OS=Homo sapiens GN=KRT3 PE=3 SV=1

Figure 4.6 – E: Evaluation of the TCC proteome post-treatment: The Venn diagram contains unique proteins for each sample. The overlapping sections represent proteins that are common to each pair of samples, or all three. The DMSO (dimethylsulfoxide) control was compared to a high dose (10 μM) and low dose (1 μM) of Firocoxib. The protein identities above are derived from the unique proteins highlighted in yellow.

5. Discussion

Canine TCC shares many similarities with its human counterpart, including etiology, drug response, and disease progression. In both species, COX-2 is a key target for clinical treatment alongside chemotherapy. The prognosis associated with canine TCC is less than a year, even with significant treatment. Typical therapeutic approaches include chemotherapeutics, such as platinum drugs or intercalating agents, alongside an NSAID. Clarification of NSAID effects independent of chemotherapy is necessary to understand the synergistic effects of this treatment.

Synthesis of PGE_2 through COX-2 has been shown to promote tumor progression through the creation of a pro-inflammatory microenvironment.[33] The autocrine and paracrine cell signaling effects of PGE_2 through its receptors (EP-1, 2, 3, and 4) can promote cell growth through various signaling pathways.[34,35] COX-2 overexpression has been correlated to aggressive cancers and poorer prognoses, which may be mediated through PGE_2 signaling.[36,37]

In our current study, we show an immense overexpression of *ptgs-2* in TCC cell lines and primary tumor samples. Such an abundance of *ptgs-2* expression leads to high expression of COX-2 protein in cancers. Interestingly, when we examined an inflamed, precancerous bladder, it exhibited a 12-fold increase in *ptgs-2* expression, which affirms the role of inflammation in cancerous processes. In other studies using canine and human models for TCC, COX-2 inhibitors display antitumor effects not only via the reduction of prostanoids and associated inflammatory response, but also through COX-2 independent mechanisms.[38,39]

Decreases in PGE_2 concentration after Firocoxib treatment *in vitro* at every concentration in both Orig and NK cell lines illustrate its efficacy of COX-2 inhibition. These data suggest the overproduction of COX-2 protein and subsequent increase in PGE_2 concentration confers resistance to NSAID treatment *in vitro*. While Firocoxib treatment successfully reduces PGE_2 concentrations, cell proliferation remains unaffected. Both canine TCC cell lines overproduce COX-2, which abrogates any decreases in PGE_2 through COX-2 inhibition. Kurtova *et al.* reports that cancer chemoresistance in bladder urothelial carcinomas occurs via PGE_2-mediated tumor repopulation post-chemotherapy, and through COX-2 inhibition, this repopulation is abolished.[40] COX-2 overproduction in canine TCC may drive formation of primary and NSAID-resistant secondary tumor populations through PGE_2 signaling. This signaling can occur through PGE_2 receptors such as EP-2, as well as through exosomal PGE_2 transcellular transport.[41] Significant elevation of PGE_2 levels in the bladder may serve as a sensitive biomarker of TCC, as it may be elevated in urine. However, elevation of this marker may accompany other inflammatory processes unassociated with neoplastic disease. Under these circumstances, the use of a highly selective COX-2 inhibitor like Firocoxib would effectively complement chemotherapy through significant reductions in PGE_2 concentration and prostanoid cell signaling.

The induction of *ptgs-2* expression can occur after cellular injury caused by ROS and other stimuli. This represents a portion of the wound response described by Kurtova *et al*.[40] Reduction of ROS production in the face of Firocoxib treatment, as seen in NK cells, may lessen the induction of *ptgs-2* and decrease PGE_2 concentrations. The difference in ROS reduction between NK and Orig cells illustrate an individualized response to Firocoxib treatment. Previous studies on NSAIDs report ROS generation through COX-independent uncoupling of oxidative phosphorylation.[42] Our data indicates that Firocoxib affects ROS generation in opposing manners in Orig and NK cells, but the precise mechanism of these effects is unknown. An overall reduction of ROS would lessen the impact of cancerous processes on the stroma, further lessening tissue injury and subsequent *ptgs-2* induction.

An increase in *vegfr1* may represent a change consistent with the previously described wound response. At the highest dose (10 μM), however, this increase does not occur, indicating that sufficient concentrations of Firocoxib effectively suppress the angiogenic response. The lack of change in proliferative index indicates that Firocoxib treatment alone does not sufficiently abrogate cell proliferation. However, the decrease in PGE_2 concentrations may modify the tumor microenvironment *in vivo*, which may affect cell proliferation. High basal *ptgs-2* expression and PGE_2 production serves as a mechanism of resistance to NSAID treatment. As noted by Sulma *et al*., higher concentrations (50 μM) will lower cell proliferation *in vitro*.[39] These concentrations cannot be reached *in vivo*, however, which suggests that COX-2 inhibition alone may not be sufficient when *ptgs-2* is overexpressed. Direct cytotoxicity must also be considered when NSAID concentration increases for *in vitro* assays. This decrease in cell proliferation may not necessarily be correlated with *ptgs-2* expression, but with other COX-2 independent mechanisms responsible for proliferation.

The canine TCC proteome underwent minimal changes. Unique proteins identified in each sample will be investigated to understand their role. In the 10 μM Firocoxib treatment, inactive caspase-12 and K-Ras-related proteins were identified. In both the 10 μM and 1 μM treatments, more Ras-related proteins, heat shock protein 75 (HSP-75), and the 75 kDa subunit of NADH-ubiquinone oxidoreductase were identified. These data suggest that the identified proteins play a role in the in vitro response to Firocoxib in canine TCC. K-Ras is associated with survival and proliferation signals, while HSP-75 and NADH-ubiquinone oxidoreductase modify ROS levels and production.[45-47] The specific role that these proteins play in canine TCC is unknown and will be investigated further.

Future research would involve more investigation the effects of *ptgs-2* overexpression in malignant TCC. This would involve examining anti-apoptotic changes mediated through Bcl-2 and suppression of caspases. The cell signaling effects PGE_2 through its receptors on healthy stromal cells and its correlation to *ptgs-2* overexpression also serve as a topic of future research. Signaling through EP receptors 1-4 has been implicated in oncogenic activity, potentially through second messengers such as cAMP-dependent protein kinase (PKA), phosphatidylinositol 3-kinase (PI3K), extraceullar signal-regulated kinases (ERK 1/2), mitogen-associated protein kinases (MAPKs), and cAMP response element-binding protein (CREB).[17,43,44] These signaling effects also may affect the cancer stroma and create a

microenvironment amenable to its proliferation. Firocoxib treatment should be performed to investigate its effects on these various pathways.

6. Conclusion

In many bladder cancers, inflammatory processes are crucial for cancer cell growth and proliferation. Increases in COX-2 activity and PGE_2 increase proliferation and promote disease progression. The inhibition of COX-2 represents a promising therapeutic target for the treatment of bladder cancers, including TCC. When considering treatment options, COX-2 selective inhibitors offer an efficacious therapy with the alleviation of adverse side effects when compared to non-specific NSAIDs.

Overexpression of *ptgs-2* was evident in all canine TCC cell lines and primary tumor samples, which underscores the importance of inflammation in cancerous process. Our study demonstrates that Firocoxib, a COX-2 inhibitor, creates significant decreases in PGE_2 concentrations *in vitro*. However, high basal *ptgs-2* expression and COX-2 activity confers resistance to NSAID treatment. This is given by the lack of change in the proliferative indexes for canine TCC with Firocoxib treatment. The TCC proteome as a whole underwent minimal changes. The role of unique proteins identified, such as K-Ras and HSP-75, are under further investigation. The quantitation of PGE_2 levels as high as 17.55 ng/mL warrants investigation into its use as a potential TCC biomarker in the urine of canines. Variable responses in oxidative stress were observed, which justifies future research to characterize metabolic effects with Firocoxib treatment. Investigation and inhibition of HSP-75 *in vitro* may clarify how Firocoxib affects oxidative stress. Future research may also focus on the role of PGE_2 receptors (EP-1 – EP-4) and its role in canine TCC. Experimental inhibition of EP receptors using siRNA or receptor antagonists is warranted. Further characterization of the effects of COX-2 inhibitors in TCC will undoubtedly benefit patients, canines and humans alike.

References

1. Mutsaers, A. J., Widmer, W. R. and Knapp, D. W. (2003), Canine Transitional Cell Carcinoma. Journal of Veterinary Internal Medicine, 17: 136–144. doi: 10.1111/j.1939-1676.2003.tb02424.x
2. Knapp, Deborah W., et al. "Cisplatin versus cisplatin combined with piroxicam in a canine model of human invasive urinary bladder cancer." *Cancer chemotherapy and pharmacology* 46.3 (2000): 221-226.
3. Khan, K. Nasir M., et al. "Expression of cyclooxygenase-2 in transitional cell carcinoma of the urinary bladder in dogs." *American journal of veterinary research* 61.5 (2000): 478-481.
4. Knapp, D. W., et al. "Randomized Trial of Cisplatin versus Firocoxib versus Cisplatin/Firocoxib in Dogs with Transitional Cell Carcinoma of the Urinary Bladder." *Journal of Veterinary Internal Medicine* 27.1 (2013): 126-133.
5. Pollmeier, M., et al. "Clinical evaluation of firocoxib and carprofen for the treatment of dogs with osteoarthritis." *Veterinary record* 159.17 (2006): 547-551.
6. Steagall, P. V. M., et al. "Evaluation of the adverse effects of oral firocoxib in healthy dogs." *Journal of veterinary pharmacology and therapeutics* 30.3 (2007): 218-223.
7. Vane, J. R., Y. S. Bakhle, and R. M. Botting. "CYCLOOXYGENASES 1 AND 2." *Annual review of pharmacology and toxicology* 38.1 (1998): 97-120.
8. Gupta, Rajnish A., and Raymond N. DuBois. "Colorectal cancer prevention and treatment by inhibition of cyclooxygenase-2." *Nature Reviews Cancer* 1.1 (2001): 11-21.
9. Crofford, L. J. "COX-1 and COX-2 tissue expression: implications and predictions." *The Journal of rheumatology. Supplement* 49 (1997): 15-19.
10. Smith, William L., David L. DeWitt, and R. Michael Garavito. "Cyclooxygenases: structural, cellular, and molecular biology." *Annual review of biochemistry* 69.1 (2000): 145-182.
11. Gierse, James K., et al. "A single amino acid difference between cyclooxygenase-1 (COX-1) and− 2 (COX-2) reverses the selectivity of COX-2 specific inhibitors." *Journal of Biological Chemistry* 271.26 (1996): 15810-15814.
12. Luong, Christine, et al. "Flexibility of the NSAID binding site in the structure of human cyclooxygenase-2." *Nature Structural & Molecular Biology* 3.11 (1996): 927-933.
13. Subbaramaiah, Kotha, and Andrew J. Dannenberg. "Cyclooxygenase 2: a molecular target for cancer prevention and treatment." *Trends in pharmacological sciences* 24.2 (2003): 96-102.
14. Dixon, Dan A., et al. "Post-transcriptional control of cyclooxygenase-2 gene expression The role of the 3′-untranslated region." *Journal of Biological Chemistry* 275.16 (2000): 11750-11757.
15. Wiese, Frederick W., Patricia A. Thompson, and Fred F. Kadlubar. "Carcinogen substrate specificity of human COX-1 and COX-2." *Carcinogenesis* 22.1 (2001): 5-10.
16. Wise, Ronald W., et al. "Metabolic activation of carcinogenic aromatic amines by dog bladder and kidney prostaglandin H synthase." *Cancer research* 44.5 (1984): 1893-1897.

17. Dempke, Wolfram, et al. "Cyclooxygenase-2: a novel target for cancer chemotherapy?." *Journal of cancer research and clinical oncology* 127.7 (2001): 411-417.
18. Carmeliet, Peter. "VEGF as a key mediator of angiogenesis in cancer." *Oncology* 69 (2004): 4-10.
19. Oshima M et al. “Suppression of intestinal polyposis in APC^{716} knock-out mice by inhibition of cyclooxygenase-2 (Cox-2).” Cell 87 (1999): 803±809
20. Ekambaram, Prasanna, et al. "Activation of thromboxane A2 receptor-alpha promotes tumor growth and angiogenesis through expression of VEGF in prostate cancer." *Cancer Research* 71.8 Supplement (2011): 3483-3483.
21. Fernandez, P. M., M. J. Manyak, and S. R. Patierno. "Effect of the cyclooxygenase-2 selective inhibitor NS398 on the secretion of matrix metalloproteinases (MMP-2 and MMP-9) and tissue inhibitors of metalloproteinase (TIMP-1 and TIMP-2) from human prostate tumor cells." *Proc Am Ass Cancer Res*. Vol. 41. 2000.
22. Dohadwala, Mariam, et al. "Autocrine/paracrine prostaglandin E2 production by non-small cell lung cancer cells regulates matrix metalloproteinase-2 and CD44 in cyclooxygenase-2-dependent invasion." *Journal of Biological Chemistry* 277.52 (2002): 50828-50833.
23. Kambayashi, Taku, et al. "Potential involvement of IL-10 in suppressing tumor-associated macrophages. Colon-26-derived prostaglandin E2 inhibits TNF-alpha release via a mechanism involving IL-10." *The Journal of Immunology* 154.7 (1995): 3383-3390.
24. Balch, C. M., et al. "Prostaglandin E2-mediated suppression of cellular immunity in colon cancer patients." *Surgery* 95.1 (1984): 71-77.
25. Pai, Rama, et al. "Prostaglandin E2 transactivates EGF receptor: a novel mechanism for promoting colon cancer growth and gastrointestinal hypertrophy." *Nature medicine* 8.3 (2002): 289-293.
26. Taketo, Makoto M. "Cyclooxygenase-2 inhibitors in tumorigenesis (part I)." *Journal of the National Cancer Institute* 90.20 (1998): 1529-1536.
27. Marnett, Lawrence J. "The COXIB experience: a look in the rearview mirror." *Annual review of pharmacology and toxicology* 49 (2009): 265-290.
28. Bergh, Mary Sarah, and Steven C. Budsberg. "The coxib NSAIDs: potential clinical and pharmacologic importance in veterinary medicine." *Journal of Veterinary Internal Medicine* 19.5 (2005): 633-643.
29. Kvaternick, V., et al. "Pharmacokinetics and metabolism of orally administered firocoxib, a novel second generation coxib, in horses." *Journal of veterinary pharmacology and therapeutics* 30.3 (2007): 208-217.
30. Mehanna, Ahmed S. "NSAIDs: chemistry and pharmacological actions." *Journal Information* 67.2 (2003).
31. Gottesman, Michael M. "Mechanisms of cancer drug resistance." *Annual review of medicine* 53.1 (2002): 615-627.
32. Longo-Sorbello, G. S. "Current understanding of methotrexate pharmacology and efficacy in acute leukemias. Use of newer antifolates in clinical trials." *haematologica* 86.2 (2001): 121-127.
33. Sinha, Pratima, et al. "Prostaglandin E2 promotes tumor progression by inducing myeloid-derived suppressor cells." *Cancer research* 67.9 (2007): 4507-4513.
34. Castellone, Maria Domenica, et al. "Prostaglandin E2 promotes colon cancer cell growth through a Gs-axin-ß-catenin signaling axis." *Science* 310.5753 (2005): 1504-1510.

35. Amano, Hideki, et al. "Host prostaglandin E2-EP3 signaling regulates tumor-associated angiogenesis and tumor growth." *The Journal of experimental medicine* 197.2 (2003): 221-232.
36. Khuri, Fadlo R., et al. "Cyclooxygenase-2 overexpression is a marker of poor prognosis in stage I non-small cell lung cancer." *Clinical Cancer Research* 7.4 (2001): 861-867.
37. Ristimäki, Ari, et al. "Prognostic significance of elevated cyclooxygenase-2 expression in breast cancer." *Cancer Research* 62.3 (2002): 632-635.
38. Knapp, Deborah W., et al. "Naturally-occurring canine transitional cell carcinoma of the urinary bladder A relevant model of human invasive bladder cancer." *Urologic Oncology: Seminars and Original Investigations*. Vol. 5. No. 2. Elsevier, 2000.
39. Mohammed, Sulma I., et al. "Cyclooxygenase inhibitors in urinary bladder cancer: in vitro and in vivo effects." *Molecular cancer therapeutics* 5.2 (2006): 329-336.
40. Kurtova, Antonina V., et al. "Blocking PGE2-induced tumour repopulation abrogates bladder cancer chemoresistance." *Nature* (2014).
41. Subra, Caroline, et al. "Exosomes account for vesicle-mediated transcellular transport of activatable phospholipases and prostaglandins." *Journal of lipid research* 51.8 (2010): 2105-2120.
42. Moreno-Sánchez, Rafael, et al. "Inhibition and uncoupling of oxidative phosphorylation by nonsteroidal anti-inflammatory drugs: Study in mitochondria, submitochondrial particles, cells, and whole heart∗∗ A preliminary report of this study was presented at the XIX ILAR Congress of Rheumatology in Singapore." *Biochemical pharmacology* 57.7 (1999): 743-752.
43. Howe, Louise R. "Cyclooxygenase/prostaglandin signaling and breast cancer." *Breast Cancer Res* 9 (2007): 210.
44. Regan, John W. "EP 2 and EP 4 prostanoid receptor signaling." *Life sciences* 74.2 (2003): 143-153.
45. Haigis, Kevin M., et al. "Differential effects of oncogenic K-Ras and N-Ras on proliferation, differentiation and tumor progression in the colon." *Nature genetics* 40.5 (2008): 600-608.
46. Hua, Guoqiang, Qixiang Zhang, and Zusen Fan. "Heat shock protein 75 (TRAP1) antagonizes reactive oxygen species generation and protects cells from granzyme M-mediated apoptosis." *Journal of Biological Chemistry* 282.28 (2007): 20553-20560.
47. Kussmaul, Lothar, and Judy Hirst. "The mechanism of superoxide production by NADH: ubiquinone oxidoreductase (complex I) from bovine heart mitochondria." *Proceedings of the National Academy of Sciences* 103.20 (2006): 7607-7612.